いて - . 新潟非小細胞肺癌学術講演会,
2009, 11, 27, 新潟. (招待講演)

H. 知的財産権の出願・登録状況(予定を含む)

1. 特許取得

なし

2. 実用新案登録

なし

3.その他

なし

研究成果の刊行に関する一覧表

雑誌

発表者氏名	論文タイトル名	発表誌名	巻号	ページ	出版年
Izawa, K., Kitaura, J., Yamanishi, Y., Matsuoka, T., Kaitani, A., Sugiuchi, M., Takahashi, M., Maehara, A., Enomoto, Y., Oki, T., Takai, T. and Kitamura, T.	Activating and inhibitory signals from an inhibitory receptor LMIR3/CLM-1: LMIR3 augments LPS response through association with FcRg in mast cells.	The Journal of Immunology	183	925-936	2009
Kawashima, T., Bao, Y.C., Minoshima, Y., Nomura, Y., Hatori, T., Hori, T., Fukagawa, T., Takahashi, N., Nosaka, T., Inoue, M., Sato, T., Kukimoto-Niino, M., Shirouzu, M., Yokoyama, S., and Kitamura, T.	A Rac GTPase activating protein MgcRacGAP is an NLS-containing nuclear chaperone in the activation of STAT transcription factors.	Molecular And Cellular Biology	29	1796-1813	2009
Islam, S.M., Shinmyo, Y., Okafuji, T., Su, Y., Naser, I.B., Ahmed, G., Zhang, S., Chen, S., Ohta, K., Kiyonari, H., Abe, T., Tanaka, S., Nishinakamura, R., Terashima, T., Kitamura, T.	Draxin, a novel repulsive guidance protein for spinal cord and forebrain commissures.	Science	323	388-393	2009

研究成果の刊行に関する一覧表

雑誌

発表者氏名	論文タイトル名	発表誌名	巻号	ページ	出版年
Ikeya M, Fukushima K, Kawada M, Onishi S, Furuta Y, Yonemura S, Kitamura T, Nosaka T, Sasai Y.	Cv2, functioning as a pro-BMP factor via twisted gastrulation, is required for early development of nephron precursors.	Developmental Biology	337	405-414	2010
Jin G, Matsushita H, Asai S, Tsukamoto H, Ono R, Nosaka T, Yahata T, Takahashi S, Miyachi H.	FLT3-ITD induces ara-C resistance in myeloid leukemic cells through the repression of the ENT1 expression.	Biochemical and Biophysical Research Communications	390	1001-1006	2009
Ono R, Kumagai H, Nakajima H, Hishiya A, Taki T, Horikawa K, Takatsu K, Satoh T, Hayashi Y, Kitamura T, Nosaka T.	Mixed-lineage-leukemia (MLL) fusion protein collaborates with Ras to induce acute leukemia through aberrant Hox expression and Raf activation.	Leukemia	23	2197-2209	2009
Watanabe-Okochi N, Oki T, Komeno Y, Kato N, Yuji K, Ono R, Harada Y, Harada H, Hayashi Y, Nakajima H, Nosaka T, Kitaura J, Kitamura T.	Possible involvement of RasGRP4 in leukemogenesis.	International Journal of Hematology	89	470-481	2009
Kawashima T, Bao YC, Minoshima Y, Nomura Y, Hatori T, Hori T, Fukagawa T, Fukada T, Takahashi N, Nosaka T, Inoue M, Sato T, Kukimoto-Niino M, Shirouzu,M, Yokoyama S, Kitamura T	Rac GTPase activating protein MgcRacGAP is an NLS-containing nuclear chaperone in the activation of STAT transcription factors.	Molecular and Cellular Biology	29	1796-1813	2009

An Activating and Inhibitory Signal from an Inhibitory Receptor LMIR3/CLM-1: LMIR3 Augments Lipopolysaccharide Response through Association with FcRγ in Mast Cells[1]

Kumi Izawa,* Jiro Kitaura,* Yoshinori Yamanishi,* Takayuki Matsuoka,* Ayako Kaitani,* Masahiro Sugiuchi,* Mariko Takahashi,* Akie Maehara,* Yutaka Enomoto,* Toshihiko Oki,* Toshiyuki Takai,† and Toshio Kitamura[2]*

Leukocyte mono-Ig-like receptor 3 (LMIR3) is an inhibitory receptor mainly expressed in myeloid cells. Coengagement of FcεRI and LMIR3 impaired cytokine production in bone marrow-derived mast cells (BMMCs) induced by FcεRI crosslinking alone. Mouse LMIR3 possesses five cytoplasmic tyrosine residues (Y241, Y276, Y289, Y303, Y325), among which Y241 and Y289 (Y241/289) or Y325 fit the consensus sequence of ITIM or immunotyrosine-based switch motif (ITSM), respectively. The inhibitory effect was abolished by the replacement of Y325 in addition to Y241/289 with phenylalanine (Y241/189/325/F) in accordance with the potential of Y241/289/325 to cooperatively recruit Src homology region 2 domain-containing phosphatase 1 (SHP)-1 or SHP-2. Intriguingly, LMIR3 crosslinking alone induced cytokine production in BMMCs expressing LMIR3 (Y241/276/289/303/325F) mutant as well as LMIR3 (Y241/289/325F). Moreover, coimmunoprecipitation experiments revealed that LMIR3 associated with ITAM-containing FcRγ. Analysis of FcRγ-deficient BMMCs demonstrated that both Y276/303 and FcRγ played a critical role in the activating function of this inhibitory receptor. Importantly, LMIR3 crosslinking enhanced cytokine production of BMMCs stimulated by LPS, while suppressing production stimulated by other TLR agonists or stem cell factor. Thus, an inhibitory receptor LMIR3 has a unique property to associate with FcRγ and thereby functions as an activating receptor in concert with TLR4 stimulation. *The Journal of Immunology,* **2009, 183: 925–936.**

The immune system is tightly regulated by the balance of activating and inhibitory signals through a variety of immune receptors. Paired immune receptors are generally composed of several activating and inhibitory receptors with high homology in the extracellular domains (1, 2). We have previously characterized leukocyte mono-Ig-like receptors 1–5 (LMIR1–5)[3] among a novel paired receptor family called LMIR/CMRF-35-like molecules (CLMs)/myeloid-associated Ig-like receptor (MAIR)/dendritic cell-derived Ig-like receptor (DIgR)/CD300 (3–9). LMIR3/CLM-1/MAIR-V/DIgR2/CD300LF is an inhibitory receptor that possesses an ITIM in the cytoplasmic region (4, 6, 7, 10, 11). On the other hand, LMIR4/CLM-5 or LMIR5/CLM-7, which is an activating receptor paired with LMIR3, associates with an ITAM-containing adaptor protein, FcRγ or DNAX activating protein of 12 kDa (DAP12), respectively (4, 11, 12). LMIR3 is mainly expressed in myeloid cells such as granulocytes, dendritic cells, and mast cells. Recent studies have demonstrated that LMIR3 is an inhibitory receptor that can block osteoclastogenesis (6), negatively regulate dendritic cell-initiated Ag-specific T cell responses (11), or impair cytokine production in mast cells (4, 6). The finding that intraperitoneal administration of LPS or G-CSF up-regulates LMIR3 in granulocytes implicates LMIR3 in innate immunity or cell differentiation (4).

Mast cells are important effector cells not only in IgE-associated allergic disorders but also in innate immunity (13–15). Several inhibitory receptors belonging to paired immune receptors are expressed in mast cells: FcγRIIB (16), gp49B1 (17), paired Ig-like receptor-B (PIR-B) (18, 19), and LMIR1/CD300A (3, 20, 21). These receptors inhibit FcεRI-mediated activating signal transduction, but how they regulate innate immune response in mast cells remains obscure.

Structurally, mouse LMIR3 contains five cytoplasmic tyrosine residues (Y241, Y276, Y289, Y303, or Y325), among which both Y241 and Y289 are located in ITIM (S/I/V/LxYxxI/V/L) and Y325 is located in the immunoreceptor tyrosine-based switch motif (ITSM) (TxYxxV/I) (22). Like ITIM, ITSM can associate with the SH2-containing tyrosine phosphatases Src homology region 2 domain-containing phosphatase 1 (SHP)-1 and SHP-2 or the SH2-containing inositol phosphatase SHIP (22, 23). On the other hand,

*Division of Cellular Therapy, Advanced Clinical Research Center, The Institute of Medical Science, The University of Tokyo, Tokyo, Japan; and the †Department of Experimental Immunology, Institute of Development, Aging and Cancer, Tohoku University, Sendai, Japan

Received for publication February 20, 2009. Accepted for publication May 18, 2009.

The costs of publication of this article were defrayed in part by the payment of page charges. This article must therefore be hereby marked *advertisement* in accordance with 18 U.S.C. Section 1734 solely to indicate this fact.

[1] This work was supported by the Ministry of Education, Science, Technology, Sports and Culture and the Ministry of Health and Welfare, Japan.

[2] Address correspondence and reprint requests to Dr. Toshio Kitamura, Division of Cellular Therapy, Advanced Clinical Research Center, The Institute of Medical Science, The University of Tokyo, 4-6-1 Shirokanedai, Minato-ku, Tokyo 108-8639, Japan. E-mail address: kitamura@ims.u-tokyo.ac.jp

[3] Abbreviations used in this paper: LMIR, leukocyte mono-Ig-like receptor; BMMC, bone marrow-derived mast cell; CLM, CMRF-35-like molecule; DAP10, DNAX activating protein of 10 kDa; IREM-1, immune receptor expressed on myeloid cells 1; ITSM, immunotyrosine-based switch motif; ODN, oligodeoxynucleotide; SHP, Src homology region 2 domain-containing phosphatase 1; SCF, stem cell factor; TNP, trinitrophenyl; WT, wild type.

www.jimmunol.org/cgi/doi/10.4049/jimmunol.0900552

unlike ITIM, ITSM binds to adaptor molecules, such as SH2-containing adaptor protein SH2 domain protein 1A (SH2D1A) and EWS-activated transcript 2 (EAT-2), as well as to Src family kinases and the p85 regulatory subunit of PI3K (22–23). Whether an ITSM transduces an activating or an inhibitory signal depends on the immune receptor and cell type. Additionally, Y276 or Y303 of LMIR3 is situated in the putative binding motif for p85 (YxxM) or Grb2 (YxN), respectively. The existence of these signaling motifs in the cytoplasmic region of LMIR3 indicates the potential of an inhibitory LMIR3 to function as an activating receptor. In fact, as recently reported by Alvarez-Errico et al., immune receptor expressed on myeloid cells 1 (IREM-1), a human homolog of mouse LMIR3, transmitted a PI3K-dependent activating signal in rat basophil leukemia (RBL) cells transduced with an IREM-1 mutant that lost inhibitory function by the replacement of several tyrosine residues with phenylalanine (24, 25). However, the biological significance of the activating function of endogenous LMIR3 remains unknown.

In the present study, we demonstrate the dual functions, inhibitory and activating, of mouse LMIR3 in mast cells. Examination of the contribution of each cytoplasmic tyrosine residue to the dual functions revealed that ITSM in addition to ITIM was required for the inhibitory function, while Y276 and Y303 were involved in the activating function. Surprisingly, LMIR3 mediated an activating signal mainly through its association with FcRγ; it is unprecedented that an ITIM-bearing receptor functions as an activating receptor by associating with an ITAM-bearing adaptor. Importantly, we delineated the biological situation where LMIR3 mediated either an inhibitory or an activating function. Notably, this positive signal of LMIR3 synergizes with TLR4 stimulation.

Materials and Methods

Abs and reagents

Rat anti-LMIR3 IgG2a mAb, designated anti-LMIR3 mAb, and goat anti-LMIR3 polyclonal Ab were obtained from R&D Systems. Anti-FLAG mAb M2, FITC-conjugated anti-FLAG mAb M2, rabbit anti-FLAG polyclonal Ab, mouse IgG1 mAb (MOPC21), and mouse anti-DNP IgE mAb (clone SPE-7; designated SPE-7 IgE) were all purchased from Sigma-Aldrich. Mouse anti-Myc mAb (9E10) was from Roche Diagnostics. Mouse anti-trinitrophenyl (TNP) IgE mAb (C38-2) and FITC-conjugated anti-mouse IgE mAb were from BD Biosciences. PE-conjugated anti-c-Kit mAb and rat IgG2a were from eBioscience. Anti-ERK, anti-Akt, anti-SH-PTP1 (C-19), anti-SH-PTP2 (C-18), anti-SHIP (N-1), and anti-Grb2 (C-23) Abs were from Santa Cruz Biotechnology. Mouse anti-phosphotyrosine mAb (4G10), rabbit anti-phosphotyrosine polyclonal Ab, rabbit anti-FcεRI-γ subunit polyclonal Ab, and rabbit anti-PI3K p85 polyclonal Ab were purchased from Upstate Biotechnology. All other phospho-specific Abs were purchased from Cell Signaling Technology. Rabbit $F(ab')_2$ anti-rat IgG(H+L) was from SouthernBiotech. Goat anti-mouse IgG(H+L) was from Zymed Laboratories. $F(ab')_2$ fragments were prepared by digesting anti-FLAG mAb M2 or mouse IgG1 mAb with immobilized pepsin, followed by removing intact mAb by protein A affinity chromatography (Pierce). Cytokines were obtained from R&D Systems. Zymosan, poly(I:C), and oligodeoxynucleotide (ODN)1585 were purchased from InvivoGen. All other reagents were from Sigma-Aldrich unless stated otherwise.

Cell culture and isolation

Ba/F3 cells and COS-7 cells were cultured as described (4). CBA/J or C57BL/6 mice (Charles River Laboratories) were used at 8–10 wk of age for isolation of cells. To generate bone marrow-derived mast cells (BMMCs) with 90% purity (c-kit$^+$/FcεRI$^+$ by flow cytometry), BMMCs were cultured in the presence of 10 ng/ml IL-3 alone or with 20 ng/ml stem cell factor (SCF), respectively, as described (4, 5, 26). The following mutant mice were used: *FcRγ*$^{-/-}$ (27).

Stimulation

In the coligation of FcεRI and endogenous LMIR3, MaxiSorp 96-well plates (Nunc, catalog no. 430341) were overnight incubated with $F(ab')_2$ anti-rat IgG Ab (SouthernBiotec), which recognized mouse IgE as well as anti-LMIR3 Ab (rat IgG2a). After BMMCs were sensitized with 0.5 μg/ml anti-TNP IgE overnight and washed twice, they were preincubated with 20 μg/ml anti-LMIR3 Ab or rat IgG2a for 1 h on ice and washed twice before stimulation with plate-coated secondary Ab. In the coligation of FcεRI and FLAG-tagged LMIR3 or LMIR1 in the transduced BMMCs, after sensitization with 0.5 μg/ml anti-TNP IgE overnight, they were preincubated with 20 μg/ml $F(ab')_2$ anti-FLAG or mouse IgG1 mAb for 1 h on ice and washed twice before stimulation with plate-coated $F(ab')_2$ anti-mouse IgG Ab (Zymed Laboratories), which recognized mouse IgE as well as $F(ab')_2$ anti-FLAG mAb (mouse IgG1). In the case of LMIR3 or LMIR1 crosslinking with or without other stimuli, LMIR was engaged by using plate-coated Ab as described in the presence or not of 10 or 100 ng/ml LPS, 100 μg/ml zymosan, 250 μg/ml poly(I:C), 5 μg/ml ODN1585, and100 ng/ml SCF. Alternatively, BMMCs were directly stimulated with 5 μg/ml SPE-7 IgE or 100 nM PMA. In the coimmunoprecipitation experiments using Ba/F3 cells, Ba/F3 cells were stimulated by 100 μM sodium pervanadate for 10 min.

Plasmid constructs

An expression plasmid encoding Myc epitope-tagged DNAX activating protein of 10 kDa (DAP10), DAP12, or FcRγ was generated as described (3–5). Signaling lymphocyte activation molecule (SLAM) signal sequence (provided by Dr. H. Arase, Osaka University) (28) Myc-DAP10, DAP12, or FcRγ fragment was subcloned into pMXs-IRES-blasticidin (pMXs-IB) (29), generating pMXs-Myc-DAP10, DAP12, or FcRγ-IB. The entire sequences excluding the leader sequence of LMIR3 and LMIR1 were amplified, and the resulting fragment was ligated into a pME vector including the signal sequence of SLAM. The resulting SLAM signal sequence-FLAG-LMIR3 or LMIR1 fragment was subcloned into pMXs-IRES-puro (pMXs-IP) generating pMXs-FLAG-LMIR3 or LMIR1-IP (29). To generate different LMIR3 mutants where one or several tyrosine residues among five cytoplasmic tyrosine residues (Y241, Y276, Y289, Y303, or Y325) are replaced with phenylalanine, two-step PCR mutagenesis was performed by using pMXs-FLAG-LMIR3 or LMIR3 mutant-IP as a template. To generate LMIR1 mutant where both Y258 and Y270 in the cytoplasmic region were replaced phenylalanine, two-step PCR mutagenesis was also performed by using pMXs-FLAG-LMIR1-IP as a template. All constructs were verified by DNA sequencing.

Transfection and infection

Retroviral transfection was as described (3–5). Briefly, retroviruses were generated by transient transfection of Plat-E packaging cells (29) with FuGENE 6 (Roche Diagnostics). Cells were infected with retroviruses in the presence of 10 μg/ml polybrene. Selection with puromycin was started 48 h after infection (30).

Biochemistry

To detect the association of LMIR3 and FcRγ, COS-7 cells were cotransfected with two constructs of interest (pMXs-FLAG-LMIR3-IP and pMXs-Myc-DAP10, DAP12, or FcRγ-IB) or (pMXs-FLAG-LMIR3 (WT), LMIR3 (Y1/3/5F), or LMIR3 (YallF)-IP and pMXs-Myc-FcRγ-IB). Cell lysis, immunoprecipitation, and Western blotting were as described (3–5).

Flow cytometry

Flow cytometric analysis of the stained cells was performed with a FACSCalibur (BD Biosciences) equipped with CellQuest software and FlowJo software (Tree Star) as described (3–5).

Measurement of cytokines

Culture supernatants of stimulated BMMCs were measured using ELISA kits of IL-6 or TNF-α from R&D Systems as described (3–5).

Statistical analysis

Data are shown as the means ± SD, and statistical significance was determined by Student's *t* test, with $p < 0.05$ taken as statistically significant.

Results

The inhibitory effect of LMIR3 on FcεRI-mediated cytokine production in mast cells

We generated BMMCs with 95% purity (FcεRI$^+$/c-kit$^+$) and confirmed surface expression of endogenous LMIR3 in BMMCs by using anti-LMIR3 Ab (Fig. 1*A*). IgE-bound FcεRI in BMMCs was engaged by plate-coated $F(ab')_2$ anti-rat IgG Ab (see *Materials*

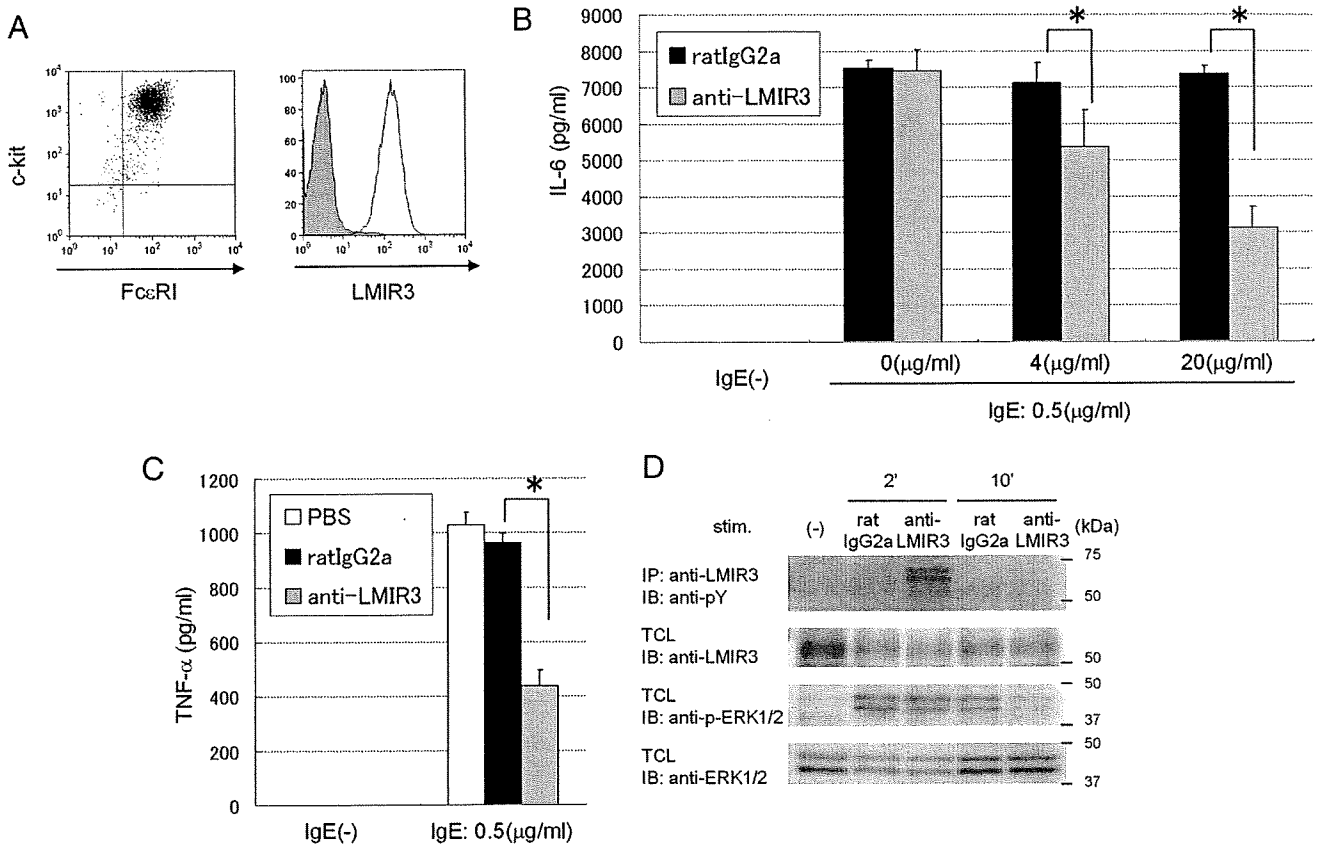

FIGURE 1. Coligation of FcεRI and LMIR3 in BMMCs impaired cytokine production induced by FcεRI crosslinking alone. *A*, Surface expression levels of c-kit and IgE-bound FcεRI (*left panel*) as well as those of endogenous LMIR3 (*right panel*) in BMMCs were analyzed by flow cytometry. *B*, IgE-bound or unbound FcεRI and endogenous LMIR3 in BMMCs were coligated by various concentrations (0, 4, 20 μg/ml) of anti-LMIR3 Ab or rat IgG2a Ab as control on $F(ab')_2$ anti-rat IgG Ab-coated plates as described in *Materials and Methods*. IL-6 released into the culture supernatants was measured by ELISA. All data points correspond to the mean and the SD of three independent experiments. Rat IgG2a or anti-LMIR3 indicates rat IgG2a Ab or rat anti-LMIR3 Ab, respectively. IgE(+) or IgE(−) indicates BMMCs sensitized with IgE or not, respectively. *C*, IgE-bound FcεRI and endogenous LMIR3 in BMMCs were coligated in BMMCs using 20 μg/ml anti-LMIR3 Ab, rat IgG2a Ab, or PBS on $F(ab')_2$ anti-rat IgG Ab-coated plates. TNF-α released into the culture supernatants was measured by ELISA. All data points correspond to the mean and the SD of three independent experiments. *D*, IgE-bound FcεRI and endogenous LMIR3 in BMMCs were coligated in BMMCs using 20 μg/ml anti-LMIR3 Ab or 20 μg/ml rat IgG2a Ab as control on $F(ab')_2$ anti-rat IgG Ab-coated plates for 2 or 10 min. Cell lysates were subjected to immunoblotting with anti-phospho-p44/42 MAPK (pERK1/2) Ab. Equal loading was evaluated by reprobing the immunoblots with anti-ERK1/2 Ab or anti-LMIR3 Ab. Immunoprecipitates of cell lysates with anti-LMIR3 Ab were immunoblotted with anti-phosphotyrosine (pY) mAb. *, $p < 0.05$.

and Methods), resulting in cytokine production of BMMCs in an IgE-dose dependent manner (supplemental Fig. S1*A*).[4] Since LMIR3 contains ITIM in the cytoplasmic region, the role of LMIR3 as an inhibitory receptor was expected in mast cells. Indeed, coligation of anti-LMIR3 Ab-bound LMIR3 and IgE-bound FcεRI in BMMCs significantly impaired the cytokine (IL-6 and TNF-α) production induced by crosslinking of IgE-bound FcεRI alone (see *Materials and Methods* and Fig. 1, *B* and *C*). No detectable cytokine production was observed in BMMCs stimulated by LMIR3 crosslinking alone (Fig. 1, *B* and *C*). Additionally, anti-LMIR3 Ab, but not control Ab, dose-dependently suppressed IL-6 production, suggesting an LMIR3-dependent inhibitory effect on FcεRI-mediated cytokine production in mast cells (Fig. 1*B*). Furthermore, Western blot analysis demonstrated increased tyrosine phosphorylation of LMIR3 at 2 min followed by attenuated ERK phosphorylation at 10 min after the coligation (Fig. 1*D*), indicating the involvement of LMIR3 cytoplasmic tyrosine residues in the inhibitory signal.

[4] The online version of this article contains supplemental material.

Y325 in addition to Y241 and Y289 played an important role in the inhibitory function of LMIR3 in mast cells

LMIR3 contains five cytoplasmic tyrosine residues, Y241, Y276, Y289, Y303, and Y325, which are hereafter abbreviated as Y1, Y2, Y3, Y4, and Y5, respectively (Fig. 2*D*). To investigate the role in the inhibitory function of each cytoplasmic tyrosine residue, we generated FLAG-tagged wild-type (WT) LMIR3 and different mutants where one or several cytoplasmic tyrosine residues were replaced with phenylalanine, as depicted in Fig. 2*D* and Table I. First, BMMCs with 95% purity ($FcεRI^+$/$c\text{-}kit^+$) were retrovirally transduced with FLAG-tagged LMIR3(WT) (Fig. 2*A*, *left panel*). Surface expression of transduced LMIR3 in BMMCs was confirmed by using anti-FLAG Ab (Fig. 2*A*, *right panel*). We also confirmed that IgE-bound FcεRI in BMMCs was engaged by plate-coated $F(ab')_2$ anti-mouse IgG Ab (see *Materials and Methods*), leading to cytokine production of BMMCs in an IgE-dose dependent manner (supplemental Fig. S1*B*). As with endogenous LMIR3, transduced FLAG-tagged LMIR3(WT) displayed an inhibitory effect on FcεRI-mediated IL-6 production and ERK activation of BMMCs (see *Materials and Methods* and Fig. 2, *B* and

Table I. *LMIR3 WT or different mutants*[a]

Abbreviation	Residues at 241, 276, 289, 303, 325
WT	Y241, Y276, Y289, Y303, Y325
Y1F	F241, Y276, Y289, Y303, Y325
Y2F	Y241, F276, Y289, Y303, Y325
Y3F	Y241, Y276, F289, Y303, Y325
Y4F	Y241, Y276, Y289, F303, Y325
Y5F	Y241, Y276, Y289, Y303, F325
Y1/3F	F241, Y276, F289, Y303, Y325
Y1/5F	F241, Y276, Y289, Y303, F325
Y3/5F	Y241, Y276, F289, Y303, F325
Y1/3/5F	F241, Y276, F289, Y303, F325
Y2/4/5F or 1/3Y	Y241, F276, Y289, F303, F325
Y2/3/4F or 1/5Y	Y241, F276, F289, F303, Y325
Y1/2/4F or 3/5Y	F241, F276, Y289, F303, Y325
Y2/4F or 1/3/5Y	Y241, F276, Y289, F303, Y325
Y2/3/4/5F or 1Y	Y241, F276, F289, F303, F325
Y1/3/4/5F or 2Y	F241, Y276, F289, F303, F325
Y1/2/4/5F or 3Y	F241, F276, Y289, F303, F325
Y1/2/3/5F or 4Y	F241, F276, F289, Y303, F325
Y1/2/3/4F or 5Y	F241, F276, F289, F303, Y325
Y1/2/3/4/5F or YallF	F241, F276, F289, F303, F325

[a] LMIR3 cytoplasmic tyrosine residues, Y241, Y276, Y289, Y303, and Y325 are abbreviated as Y1, Y2, Y3, Y4, and Y5, respectively. In LMIR3 mutants, single or several tyrosine residues (Y) were replaced with phenylalanine (F).

Y4 are not important for the inhibitory function of LMIR3. On the other hand, LMIR3(Y1F), (Y3F), or (Y5F) mutant-mediated inhibition was only 45–60% when compared with LMIR3(WT)-mediated inhibition. In the LMIR3(Y1/3F) mutant where both Y1 and Y3 located in ITIM were replaced with phenylalanine, the inhibition was 30%. Coligation of FcεRI and LMIR3(Y1/3/5F) mutant, where Y5 located in ITSM in addition to Y1/3 was replaced with phenylalanine, did not result in the inhibition of IL-6 production at all. Collectively, these results indicated that the inhibitory effect of LMIR3 on FcεRI-mediated cytokine production was dependent on both ITIM and ITSM in the cytoplasmic region.

LMIR3 associated with SHP-1 and SHP-2 via phosphorylated Y241, Y289, and Y325, while associating with the p85 subunit of PI3K via phosphorylated Y276

We next explored which molecules LMIR3 associated with through the phosphorylation of its cytoplasmic tyrosine residues. When FLAG-tagged LMIR3(WT)-transduced Ba/F3 cells were stimulated by sodium pervanadate, Western blot analysis displayed a mobility shift of tyrosine-phosphorylated LMIR3 (Fig. 3*A*, *left panel*). Generally, ITIM can associate with phosphatases such as SHP-1, SHP-2, or SHIP, while ITSM can bind not only to phosphatases but also to the p85 regulatory subunit of PI3K or to other adaptor molecules, depending on receptor type and cellular context (22, 23). Moreover, Y276 or Y303 fits the putative binding motif for p85 or Grb2, respectively. Therefore, we performed coimmunoprecipitation experiments using LMIR3(WT)-transduced Ba/F3 cells stimulated by sodium pervanadate. Immunoprecipitates of lysates with anti-FLAG Ab were subjected to probing with anti-SHP-1, SHP-2, SHIP, p85, or Grb2 Ab, demonstrating that tyrosine-phosphorylated LMIR3 associated with SHP-1 or SHP-2, but not with SHIP, among phosphatases, and with p85 or Grb2 (Fig. 3*A*, *middle panel*). Because Grb2 was not easy to discern from the nonspecific Ig L chain due to the similar mobilities in the Western blot, immunoprecipitates of lysates with anti-Grb2 Ab were also probed with anti-LMIR3 Ab, confirming that Grb2 associated with phosphorylated LMIR3 (Fig. 3*A*, *right panel*). Moreover, similar results that tyrosine-phosphorylated LMIR3 associated with SHP-1, SHP-2, or p85 were also obtained by coimmunoprecipitation experiments using LMIR3(WT)-transduced BMMCs (supplemental Fig. S3). To further explore the contribution of each tyrosine residue to the association of LMIR3 with SHP-1, SHP-2, or p85, different LMIR3 mutant-transduced Ba/F3 cells were generated. Equivalent expression levels of surface LMIR3 were confirmed among different transfectants by using anti-FLAG Ab (supplemental Fig. 4). We also performed coimmunoprecipitation experiments on Ba/F3 transfectants expressing the mutants. The association of LMIR3 with SHP-1, SHP-2, or p85 as well as tyrosine phosphorylation and concomitant mobility shift of LMIR3 upon sodium pervanadate stimulation was abolished by the replacement of all five tyrosine residues with phenylalanine in the cytoplasmic LMIR3 (Fig. 3*B*, *left panel*). This confirmed that tyrosine phosphorylation of LMIR3 was necessary for the association of LMIR3 with SHP-1, SHP-2, or p85. As shown in Fig. 3*B*, only LMIR3(Y2F) mutant did not coimmunoprecipitate p85 among LMIR3 mutants where a single tyrosine residue was replaced with phenylalanine (*left panel*). In parallel, only LMIR3(2Y) mutant coimmunoprecipitated p85 among LMIR3 mutants where four of five tyrosine residues were replaced with phenylalanine, at levels comparable to LMIR3(WT) (Fig. 3*B*, *right panel*). Thus, Y276 was indispensable for the association of LMIR3 with p85. On the other hand, the association of LMIR3 with SHP-1 or SHP-2 was slightly reduced in LMIR3(Y1F), (Y3F), or (Y5F) mutants (Fig. 3*B*, *right panel*), while LMIR3(1Y), (3Y), or (5Y) mutant did not coimmunoprecipitate SHP-1 or SHP-2 at all (Fig. 3*B*, *right panel*). These results suggested that the combination of Y1, Y3, or Y5 is required for the association. Analysis of LMIR3(Y1/3F), (Y1/5F), (Y3/5F), (Y1/3/5F), (1/3Y), (1/5Y), (3/5Y), or (1/3/5Y) mutant demonstrated that Y1/3/5(> Y1/5 > Y3/5 > Y1/3 in order) played a critical role in the association of LMIR3 with SHP-1 or SHP-2 (Fig. 3*C*), which was in accordance with the finding that Y1, Y3, and Y5 are required for the maximum inhibitory effect of LMIR3 on FcεRI-mediated cytokine production (Fig. 2*E*).

Crosslinking of LMIR3(Y241/276/289/303/325/F) mutant as well as LMIR3(Y241/289/325/F) mutant resulted in IL-6 production in the transduced BMMCs

The potential of LMIR3 to associate with p85 or Grb2 via its tyrosine phosphorylation prompted us to postulate that LMIR3 could transmit an activating signal, at least in LMIR3 mutants that lost the inhibitory function. In fact, cytokine production of the transduced BMMCs was strongly induced by crosslinking of LMIR3(Y1/3/5F) mutant that had lost the inhibitory function (Fig. 4*A*). Consistently, engagement of LMIR3(Y1/3F) mutant that partially lost the inhibitory function resulted in lower but significant levels of IL-6 production compared with that of LMIR3(Y1/3/5F) mutant (Fig. 4*A*). Moreover, Western blot analysis demonstrated that crosslinking of LMIR3(Y1/3/5F) in the transduced BMMCs induced the tyrosine phosphorylation of LMIR3 and the association of LMIR3 with p85, suggesting the importance of Y2 and Y4 in the activating role of LMIR3 (Fig. 4*C*). In contrast, cytokine production was not significantly induced by crosslinkng of LMIR3(WT) or LMIR3(Y1F), (Y2F), (Y3F), (Y4F), (Y5F), (Y2/4F), or (Y2/4/5F) mutants (Fig. 4*A*). Collectively, these results are consistent with the finding recently reported by Alvarez-Errico et al. on IREM-1/human LMIR3 that both Y236 and Y263 in IREM-1 played an important part in IREM-1-mediated activating signal (25). Furthermore, similar experiments were conducted on LMIR1, another ITIM-containing receptor among the LMIR family. In BMMCs transduced with LMIR1(WT) or LMIR1(Y258/270F) mutant in which the inhibitory function was disrupted by the replacement

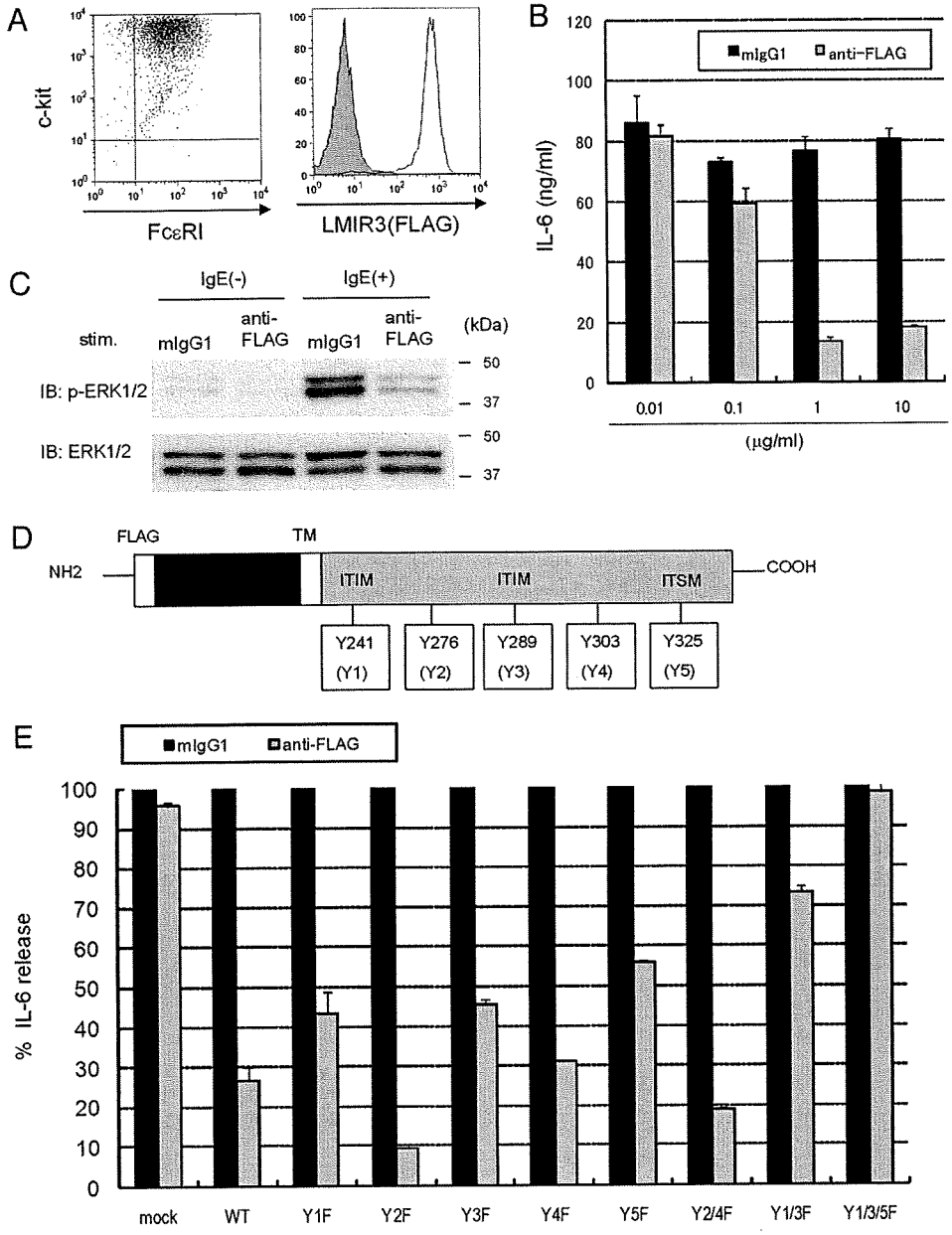

FIGURE 2. LMIR3 transmits an inhibitory signal in BMMCs via Y325 located in ITSM in addition to Y241/Y289 located in ITIM. *A*, BMMCs from mice were transduced with FLAG-tagged LMIR3. Surface expression levels of c-kit and IgE-bound FcεRI as well as those of FLAG-tagged LMIR3 were analyzed by flow cytometry. *B*, IgE-bound FcεRI and FLAG-tagged LMIR3 in the transduced BMMCs were coligated by using various concentrations (0, 0.1, 1, 10 μg/ml) of $F(ab')_2$ anti-FLAG mAb or mouse IgG1 mAb as control on $F(ab')_2$ anti-mouse IgG Ab-coated plates as described in *Materials and Methods*. IL-6 released into the culture supernatants was measured by ELISA. All data points correspond to the mean and the SD of three independent experiments. mIgG1 or anti-FLAG indicates $F(ab')_2$ mouse IgG1 mAb or $F(ab')_2$ anti-FLAG mAb. *C*, IgE-bound or unbound FcεRI and FLAG-tagged LMIR3 in the transduced BMMCs were coligated by 10 μg/ml $F(ab')_2$ anti-FLAG mAb or 10 μg/ml mouse IgG1 mAb as control on $F(ab')_2$ anti-mouse IgG Ab-coated plates for 10 min. Cell lysates were subject to immunoblotting with anti-phospho-p44/42 MAPK (pERK1/2) Ab. Equal loading was evaluated by reprobing the immunoblot with anti-ERK1/2 Ab. IgE(+) or IgE(−) indicates BMMCs sensitized with IgE or not, respectively. *D*, Structure of FLAG-tagged LMIR3(WT) containing cytoplasmic five tyrosine residues, Y241, Y276, Y289, Y303, and Y325, abbreviated as Y1, Y2, Y3, Y4, and Y5, respectively. Y1 and Y3 are located in ITIM, while Y5 is located in ITSM. TM indicates the transmembrane region. *E*, The ratio of the amounts of IL-6 produced by each transfectant when FLAG-tagged LMIR3 mutant and IgE-bound FcεRI were coligated by using $F(ab')_2$ anti-FLAG mAb to those only when IgE-bound FcεRI was engaged by using $F(ab')_2$ mouse IgG1 mAb. BMMCs were transduced with FLAG-tagged LMIR3(WT), different mutants, or mock. Data are representative of three independent experiments. All data points correspond to the mean and the SD.

C). Next, we generated different LMIR3 mutant-transduced BMMCs that showed equivalent levels of mast cell maturity and surface LMIR3 expression, although higher expression levels of LMIR3 were observed in LMIR3(YallF) mutant-transduced BMMCs (supplemental Fig. S2). To examine the inhibitory effect of each LMIR3 mutant, we measured the ratio of the amounts of IL-6 produced by each transfectant when FLAG-tagged LMIR3 mutants and FcεRI were coligated to those when FcεRI was engaged alone, as described in *Materials and Methods*. As demonstrated in Fig. 2*E*, LMIR3(WT)-mediated inhibition of IL-6 production was ~75%. Among LMIR3 mutants, LMIR3(Y2F), (Y4F), or (Y2/4F) mutant-mediated inhibition was 70–90%, indicating that Y2 and

Table I. *LMIR3 WT or different mutants*[a]

Abbreviation	Residues at 241, 276, 289, 303, 325
WT	Y241, Y276, Y289, Y303, Y325
Y1F	F241, Y276, Y289, Y303, Y325
Y2F	Y241, F276, Y289, Y303, Y325
Y3F	Y241, Y276, F289, Y303, Y325
Y4F	Y241, Y276, Y289, F303, Y325
Y5F	Y241, Y276, Y289, Y303, F325
Y1/3F	F241, Y276, F289, Y303, Y325
Y1/5F	F241, Y276, Y289, Y303, F325
Y3/5F	Y241, Y276, F289, Y303, F325
Y1/3/5F	F241, Y276, F289, Y303, F325
Y2/4/5F or 1/3Y	Y241, F276, Y289, F303, F325
Y2/3/4F or 1/5Y	Y241, F276, F289, F303, Y325
Y1/2/4F or 3/5Y	F241, F276, Y289, F303, Y325
Y2/4F or 1/3/5Y	Y241, F276, Y289, F303, Y325
Y2/3/4/5F or 1Y	Y241, F276, F289, F303, F325
Y1/3/4/5F or 2Y	F241, Y276, F289, F303, F325
Y1/2/4/5F or 3Y	F241, F276, Y289, F303, F325
Y1/2/3/5F or 4Y	F241, F276, F289, Y303, F325
Y1/2/3/4F or 5Y	F241, F276, F289, F303, Y325
Y1/2/3/4/5F or YallF	F241, F276, F289, F303, F325

[a] LMIR3 cytoplasmic tyrosine residues, Y241, Y276, Y289, Y303, and Y325 are abbreviated as Y1, Y2, Y3, Y4, and Y5, respectively. In LMIR3 mutants, single or several tyrosine residues (Y) were replaced with phenylalanine (F).

Y4 are not important for the inhibitory function of LMIR3. On the other hand, LMIR3(Y1F), (Y3F), or (Y5F) mutant-mediated inhibition was only 45–60% when compared with LMIR3(WT)-mediated inhibition. In the LMIR3(Y1/3F) mutant where both Y1 and Y3 located in ITIM were replaced with phenylalanine, the inhibition was 30%. Coligation of FcεRI and LMIR3(Y1/3/5F) mutant, where Y5 located in ITSM in addition to Y1/3 was replaced with phenylalanine, did not result in the inhibition of IL-6 production at all. Collectively, these results indicated that the inhibitory effect of LMIR3 on FcεRI-mediated cytokine production was dependent on both ITIM and ITSM in the cytoplasmic region.

LMIR3 associated with SHP-1 and SHP-2 via phosphorylated Y241, Y289, and Y325, while associating with the p85 subunit of PI3K via phosphorylated Y276

We next explored which molecules LMIR3 associated with through the phosphorylation of its cytoplasmic tyrosine residues. When FLAG-tagged LMIR3(WT)-transduced Ba/F3 cells were stimulated by sodium pervanadate, Western blot analysis displayed a mobility shift of tyrosine-phosphorylated LMIR3 (Fig. 3*A*, *left panel*). Generally, ITIM can associate with phosphatases such as SHP-1, SHP-2, or SHIP, while ITSM can bind not only to phosphatases but also to the p85 regulatory subunit of PI3K or to other adaptor molecules, depending on receptor type and cellular context (22, 23). Moreover, Y276 or Y303 fits the putative binding motif for p85 or Grb2, respectively. Therefore, we performed coimmunoprecipitation experiments using LMIR3(WT)-transduced Ba/F3 cells stimulated by sodium pervanadate. Immunoprecipitates of lysates with anti-FLAG Ab were subjected to probing with anti-SHP-1, SHP-2, SHIP, p85, or Grb2 Ab, demonstrating that tyrosine-phosphorylated LMIR3 associated with SHP-1 or SHP-2, but not with SHIP, among phosphatases, and with p85 or Grb2 (Fig. 3*A*, *middle panel*). Because Grb2 was not easy to discern from the nonspecific Ig L chain due to the similar mobilities in the Western blot, immunoprecipitates of lysates with anti-Grb2 Ab were also probed with anti-LMIR3 Ab, confirming that Grb2 associated with phosphorylated LMIR3 (Fig. 3*A*, *right panel*). Moreover, similar results that tyrosine-phosphorylated LMIR3 associated with SHP-1, SHP-2, or p85 were also obtained by coimmunoprecipitation experiments using LMIR3(WT)-transduced BMMCs (supplemental Fig. S3). To further explore the contribution of each tyrosine residue to the association of LMIR3 with SHP-1, SHP-2, or p85, different LMIR3 mutant-transduced Ba/F3 cells were generated. Equivalent expression levels of surface LMIR3 were confirmed among different transfectants by using anti-FLAG Ab (supplemental Fig. 4). We also performed coimmunoprecipitation experiments on Ba/F3 transfectants expressing the mutants. The association of LMIR3 with SHP-1, SHP-2, or p85 as well as tyrosine phosphorylation and concomitant mobility shift of LMIR3 upon sodium pervanadate stimulation was abolished by the replacement of all five tyrosine residues with phenylalanine in the cytoplasmic LMIR3 (Fig. 3*B*, *left panel*). This confirmed that tyrosine phosphorylation of LMIR3 was necessary for the association of LMIR3 with SHP-1, SHP-2, or p85. As shown in Fig. 3*B*, only LMIR3(Y2F) mutant did not coimmunoprecipitate p85 among LMIR3 mutants where a single tyrosine residue was replaced with phenylalanine (*left panel*). In parallel, only LMIR3(2Y) mutant coimmunoprecipitated p85 among LMIR3 mutants where four of five tyrosine residues were replaced with phenylalanine, at levels comparable to LMIR3(WT) (Fig. 3*B*, *right panel*). Thus, Y276 was indispensable for the association of LMIR3 with p85. On the other hand, the association of LMIR3 with SHP-1 or SHP-2 was slightly reduced in LMIR3(Y1F), (Y3F), or (Y5F) mutants (Fig. 3*B*, *right panel*), while LMIR3(1Y), (3Y), or (5Y) mutant did not coimmunoprecipitate SHP-1 or SHP-2 at all (Fig. 3*B*, *right panel*). These results suggested that the combination of Y1, Y3, or Y5 is required for the association. Analysis of LMIR3(Y1/3F), (Y1/5F), (Y3/5F), (Y1/3/5F), (1/3Y), (1/5Y), (3/5Y), or (1/3/5Y) mutant demonstrated that Y1/3/5(> Y1/5 > Y3/5 > Y1/3 in order) played a critical role in the association of LMIR3 with SHP-1 or SHP-2 (Fig. 3*C*), which was in accordance with the finding that Y1, Y3, and Y5 are required for the maximum inhibitory effect of LMIR3 on FcεRI-mediated cytokine production (Fig. 2*E*).

Crosslinking of LMIR3(Y241/276/289/303/325/F) mutant as well as LMIR3(Y241/289/325/F) mutant resulted in IL-6 production in the transduced BMMCs

The potential of LMIR3 to associate with p85 or Grb2 via its tyrosine phosphorylation prompted us to postulate that LMIR3 could transmit an activating signal, at least in LMIR3 mutants that lost the inhibitory function. In fact, cytokine production of the transduced BMMCs was strongly induced by crosslinking of LMIR3(Y1/3/5F) mutant that had lost the inhibitory function (Fig. 4*A*). Consistently, engagement of LMIR3(Y1/3F) mutant that partially lost the inhibitory function resulted in lower but significant levels of IL-6 production compared with that of LMIR3(Y1/3/5F) mutant (Fig. 4*A*). Moreover, Western blot analysis demonstrated that crosslinking of LMIR3(Y1/3/5F) in the transduced BMMCs induced the tyrosine phosphorylation of LMIR3 and the association of LMIR3 with p85, suggesting the importance of Y2 and Y4 in the activating role of LMIR3 (Fig. 4*C*). In contrast, cytokine production was not significantly induced by crosslinkng of LMIR3(WT) or LMIR3(Y1F), (Y2F), (Y3F), (Y4F), (Y5F), (Y2/4F), or (Y2/4/5F) mutants (Fig. 4*A*). Collectively, these results are consistent with the finding recently reported by Alvarez-Errico et al. on IREM-1/human LMIR3 that both Y236 and Y263 in IREM-1 played an important part in IREM-1-mediated activating signal (25). Furthermore, similar experiments were conducted on LMIR1, another ITIM-containing receptor among the LMIR family. In BMMCs transduced with LMIR1(WT) or LMIR1(Y258/270F) mutant in which the inhibitory function was disrupted by the replacement

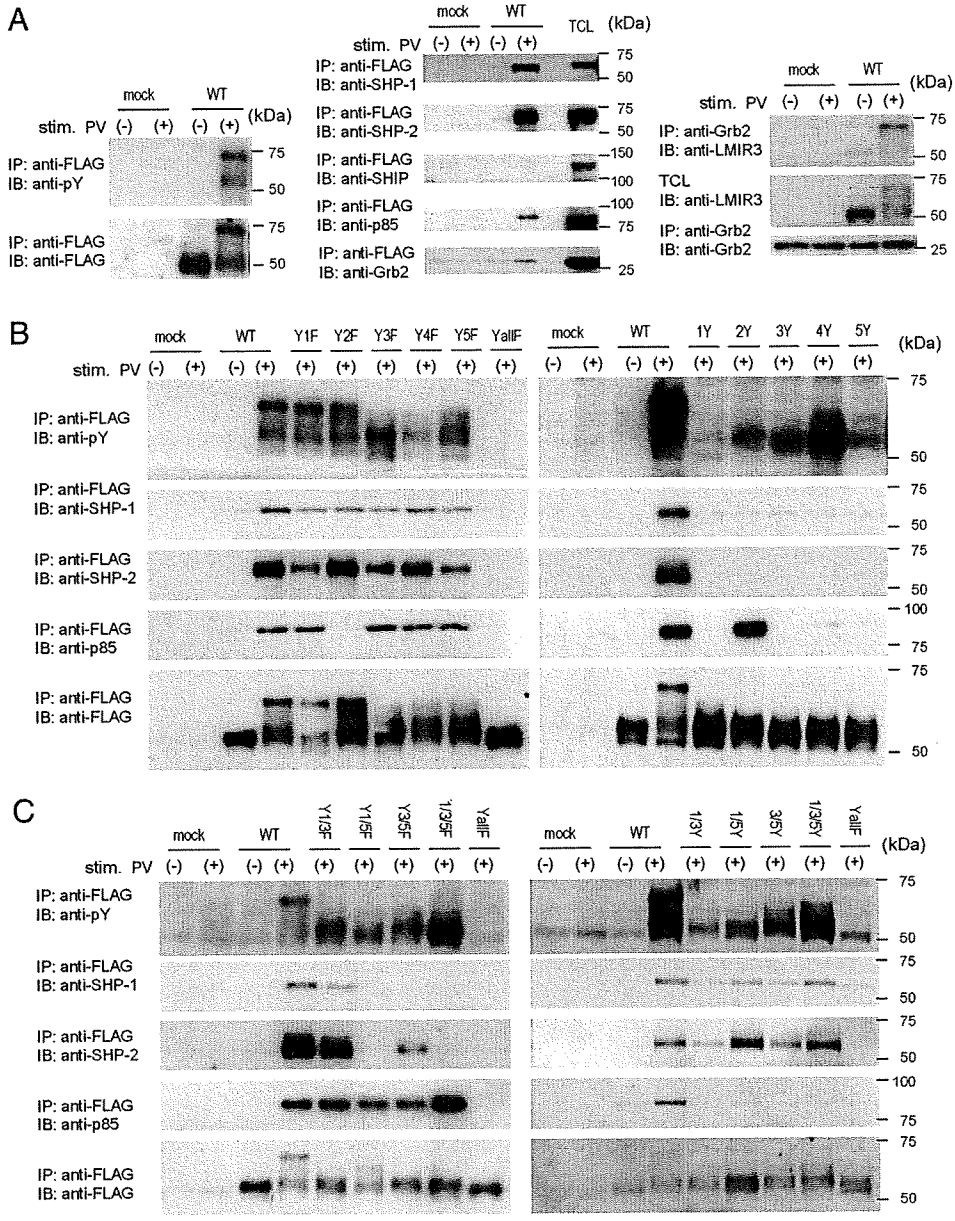

FIGURE 3. LMIR3 associates with SHP-1 or SHP-2 via Y241/289/325, while it does so with p85α via Y276. *A*, Ba/F3 cells transduced with FLAG-tagged LMIR3(WT) or mock were stimulated or not with 100 μM sodium pervanadate. Immunoprecipitates of cell lysates with rabbit anti-FLAG Ab or total cell lysates were blotted with anti-phosphotyrosine (pY) mAb or anti-FLAG mAb (*left panel*), anti-SHP-1 Ab, anti-SHP-2 Ab, anti-SHIP Ab, anti-p85 Ab, or anti-Grb2 Ab (*middle panel*). Alternatively, immunoprecipitates of cell lysates with anti-Grb2 Ab were blotted with anti-LMIR3 Ab or anti-Grb2 Ab, and total cell lysates were blotted with anti-LMIR3 Ab (*right panel*). *B* and *C*, Ba/F3 cells transduced with FLAG-tagged LMIR3 WT, different mutants, or mock were stimulated or not with 100 μM sodium pervanadate. Immunoprecipitates of cell lysates with rabbit anti-FLAG Ab were blotted with anti-pY mAb, anti-SHP-1 Ab, anti-SHP-2 Ab, anti-p85 Ab, or anti-FLAG mAb. *B*, Ba/F3 cells transduced with FLAG-tagged LMIR3(WT), (Y1F), (Y2F), (Y3F), (Y4F), (Y5F), or mock (*left panel*) or with FLAG-tagged LMIR3(WT), (1Y), (2Y), (3Y), (4Y), (5Y), or mock (*right panel*) were used. *C*, Ba/F3 cells transduced with LMIR3(WT), (Y1/3F), (Y1/5F), (Y3/5F), (Y1/3/5F), (YallF), or mock (*left panel*) or with LMIR3(WT), (1/3Y), (1/5Y), (3/5Y), (1/3/5Y), (YallF), or mock (*right panel*) were used. Data are representative of three independent experiments. TCL and VO_4 indicate total cell lysates and sodium pervanadate, respectively.

of both Y258 and Y270 situated in ITIM with phenylalanine (21), comparable surface expression levels of LMIR1 as well as mast cell maturity were confirmed as well (supplemental Fig. 2). When either transfectant was stimulated by LMIR1 crosslinking, we found no detectable levels of cytokine production (Fig. 4*A*), indicating the specificity of LMIR3-mediated activation events. However, unlike the results for IREM-1, crosslinking of LMIR3(YallF) mutant that did not contain phosphorylatable tyrosine residues led to the production of a significant level of IL-6 in the transduced BMMCs. These results let us postulate the potential of LMIR3 to transmit an activating signal independent of its cytoplsmic tyrosine residues.

LMIR3 associated with FcRγ, but not DAP10 or DAP12, in BMMCs

To clarify the mechanism of LMIR3-mediated activating signal independent of LMIR3 tyrosine phosphorylation (Fig. 4*A*), we attempted to test the possibility that LMIR3 associated with FcRγ, DAP10, or DAP12, although it was unlikely that ITIM-containing inhibitory receptors associated with ITAM- or the related activating motif-bearing adaptor molecules. Surprisingly, coimmunoprecipitation experiments using COS-7 cells cotransduced with LMIR3(WT) and either Myc-tagged FcRγ, DAP10, DAP12, or mock clearly demonstrated that LMIR3 associated with FcRγ, but not DAP10 or DAP12 (Fig. 4*B*, *left panel*). Similar coimmunoprecipitation experiments also revealed that not only LMIR3(WT) but also LMIR3(Y1/3/5F) or LMIR3(YallF) mutant associated with FcRγ (Fig. 4*B*, *right panel*), suggesting that the association of LMIR3 with FcRγ was independent of tyrosine residues of LMIR3. Additionally, in either WT or FcRγ-deficient BMMCs transduced with LMIR3(WT), (Y1/3/5F) mutant, or (YallF) mutant, we confirmed the association of LMIR3, irrespective of WT or mutants, with endogenous FcRγ in mast cells (Fig. 4*D*). Collectively, an inhibitory receptor LMIR3 associated with FcRγ in mast cells.

FcRγ played a critical role in LMIR3-mediated cytokine production in LMIR3(Y241/289/325F) or (Y241/276/289/303/325F) mutant-transduced BMMCs

As shown in Fig. 5*A*, equivalent surface expression levels of c-kit with no detectable FcεRI were observed in FcRγ-deficient

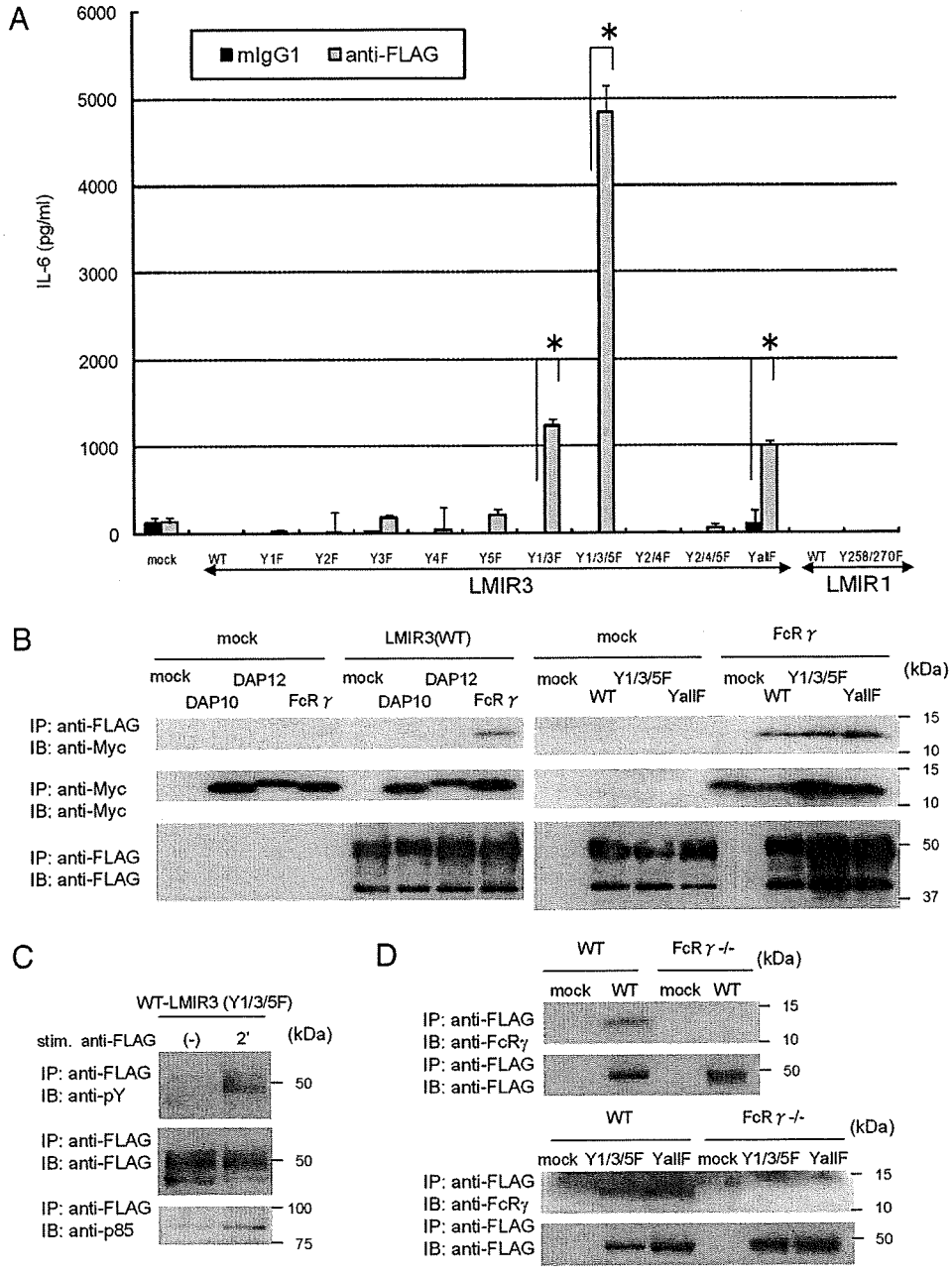

FIGURE 4. Crosslinking of LMIR3-(Y241/289/325F) or LMIR3(Y241/276/289/303/325F) in the transduced BMMCs induced cytokine production. *A*, BMMCs transduced with FLAG-tagged LMIR3(WT), (Y1F), (Y2F), (Y3F), (Y4F), (Y5F), (Y1/3F), (Y1/3/5F), (Y2/4F), (Y2/4/5F), or (YallF), FLAG-tagged LMIR1(WT) or (YF), or mock were stimulated by using 10 μg/ml $F(ab')_2$ anti-FLAG mAb or 10 μg/ml mouse IgG1 mAb as control. IL-6 released into the culture supernatants was measured by ELISA. All data points correspond to the mean and the SD of three independent experiments. *, $p < 0.05$. *B*, COS-7 cells were transiently cotransduced with a Myc-tagged DAP10, DAP12, or FcRγ or mock and a FLAG-tagged LMIR3 or mock (*left panel*), or a Myc-tagged FcRγ or mock and a FLAG-tagged LMIR3(WT), (Y1/3/5F), or (YallF) or mock (*right panel*). Immunoprecipitates of lysates of these transfectants with anti-FLAG mAb were probed with anti-Myc or anti-FLAG mAb. Immunoprecipitates of the same series of lysates with anti-Myc mAb were also probed with anti-Myc mAb. One representative of three independent experiments is shown. *C*, LMIR3(Y1/3/5F)-transduced BMMCs were stimulated by using $F(ab')_2$ anti-FLAG mAb for 2 min. Immunoprecipitates of cell lysates were blotted with anti-pY mAb or anti-p85 Ab. Equal loading was evaluated by reprobing immunoblots with anti-FLAG mAb. One representative of three independent experiments is shown. *D*, WT or FcRγ-deficient BMMCs were transduced with FLAG-tagged LMIR3(WT), (Y1/3/5F), (YallF), or mock. Immunoprecipitates of cell lysates with anti-FLAG Ab were blotted with anti-FcRγ Ab. Equal loading was evaluated by reprobing immunoblots with anti-FLAG mAb. One representative of three independent experiments is shown.

BMMCs transduced with LMIR3(WT), (Y1/3/5F) mutant, (YallF) mutant, or mock (26). When surface expression levels of LMIR3(WT) or mutants were compared between WT and FcRγ-deficient BMMCs, no significant difference was observed, suggesting that FcRγ was dispensable for efficient surface expression of LMIR3 in BMMCs despite its association with LMIR3 (Fig. 5*A*). To clarify the role of FcRγ in the activating function of LMIR3, we measured the amounts of IL-6 released from LMIR3(Y1/3/5F)-transduced WT or FcRγ-deficient BMMCs stimulated by LMIR3 crosslinking. Notably, the deficiency of FcRγ severely, but not completely, impaired IL-6 production of the transduced BMMCs stimulated by LMIR3 crosslinking. As expected, the deficiency of FcRγ completely abolished IgE-dependent IL-6 production, although PMA stimulation led to comparable amounts of IL-6 production in both transfectants (Fig. 5*B*). In accordance with this, FcRγ deficiency caused severe impairment of both ERK and Akt activation in the transduced BMMCs stimulated by crosslinking of LMIR3(Y1/3/5F) (Fig. 5*C*). Next, similar experiments were performed in WT and FcRγ-deficient BMMCs transduced with LMIR3(YallF) mutant. Strikingly, the absence of FcRγ completely dampened IL-6 production of the transduced BMMCs stimulated by crosslinking of LMIR3(YallF) mutant as well as by IgE, although PMA as a control produced comparable levels of IL-6 irrespective of the presence or absence of FcRγ (Fig. 5*D*). Collectively, these results suggested that FcRγ played a predominant role in cytokine production of BMMCs stimulated by crosslinking of LMIR3(Y1/3/5F) or (YallF) mutant.

Crosslinking of LMIR3 enhanced cytokine production of BMMCs triggered by TLR4 agonist, while it suppressed that stimulated by other TLR agonists or SCF

Since the potential of LMIR3 to transmit an activating signal in mast cells had been demonstrated, we next attempted to find the physiological situation where LMIR3 functions as an activating receptor. Intriguingly, crosslinking of LMIR3 dramatically enhanced cytokine production of LMIR3(WT)-transduced BMMCs

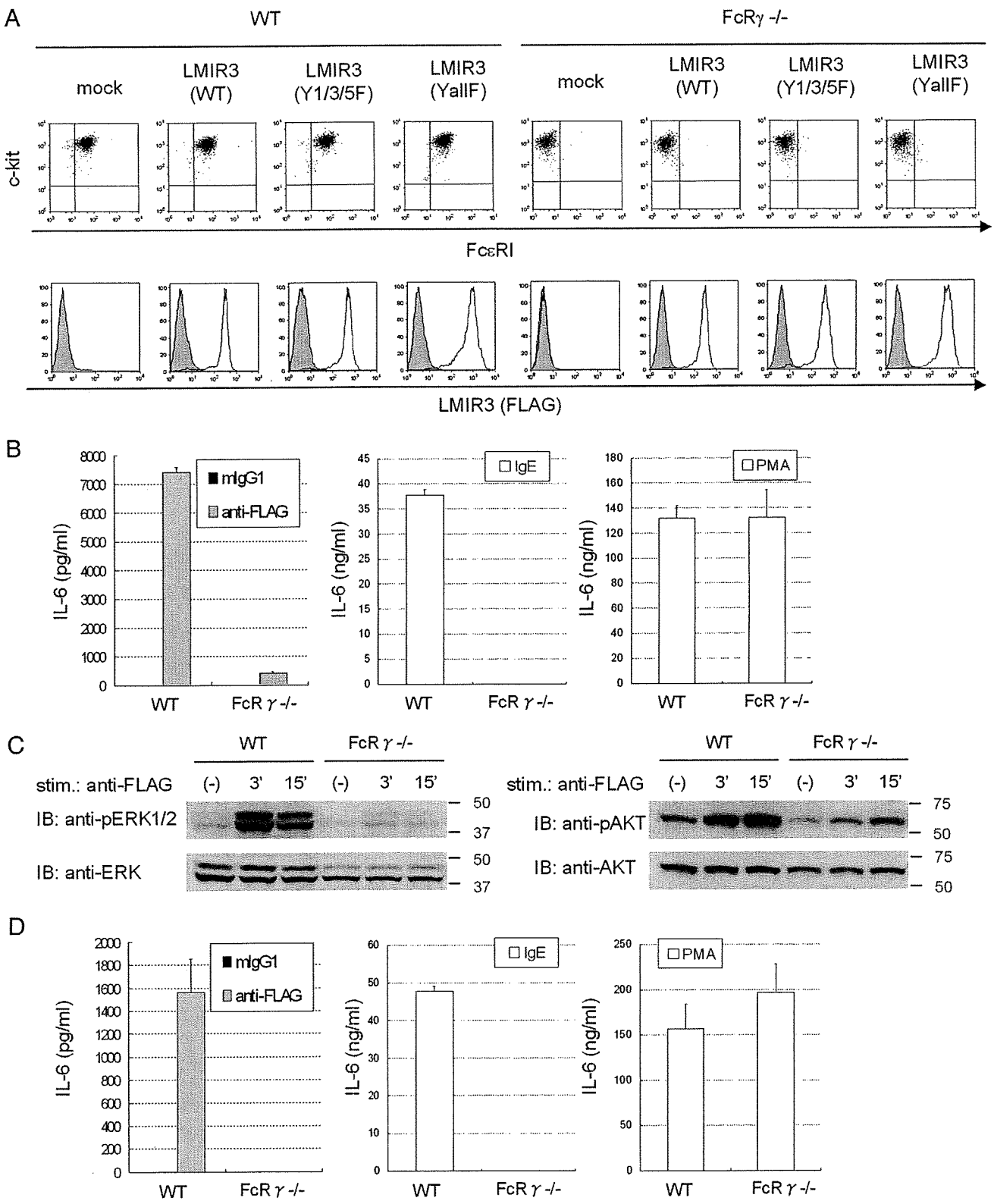

FIGURE 5. Cytokine production of the transduced BMMCs induced by engagement of LMIR3(Y241/289/325F) or LMIR3(Y241/276/289/303/325F) is severely or completely, respectively, impaired by FcRγ deficiency. *A*, WT or FcRγ-deficient BMMCs were transduced with FLAG-tagged LMIR3(WT), (Y1/3/5F) mutant, (YallF) mutant, or mock. Surface expression levels of c-kit and IgE-bound FcεRI as well as those of FLAG-tagged LMIR3 were analyzed by flow cytometry. *B* and *D*, WT or FcRγ-deficient BMMCs transduced with LMIR3(Y1/3/5F) (*B*) or LMIR3(YallF) (*D*) were stimulated by $F(ab')_2$ anti-FLAG mAb or $F(ab')_2$ mouse IgG1 as control (*left panel*), SPE-7 IgE (*middle panel*), or PMA (*right panel*). IL-6 released into the culture supernatants was measured by ELISA. All data points correspond to the mean and the SD of four independent experiments. *C*, WT or FcRγ-deficient BMMCs transduced with LMIR3(Y1/3/5F) were stimulated by $F(ab')_2$ anti-FLAG mAb for the indicated times. Cell lysates were subject to immunoblotting with anti-phospho-p44/42 MAPK (pERK1/2) Ab (*left panel*) or anti-phospho-Akt Ab (*right panel*). Equal loading was evaluated by reprobing the immunoblots with anti-ERK1/2 Ab (*left panel*) or anti-Akt Ab (*right panel*). One representative of three independent experiments is shown.

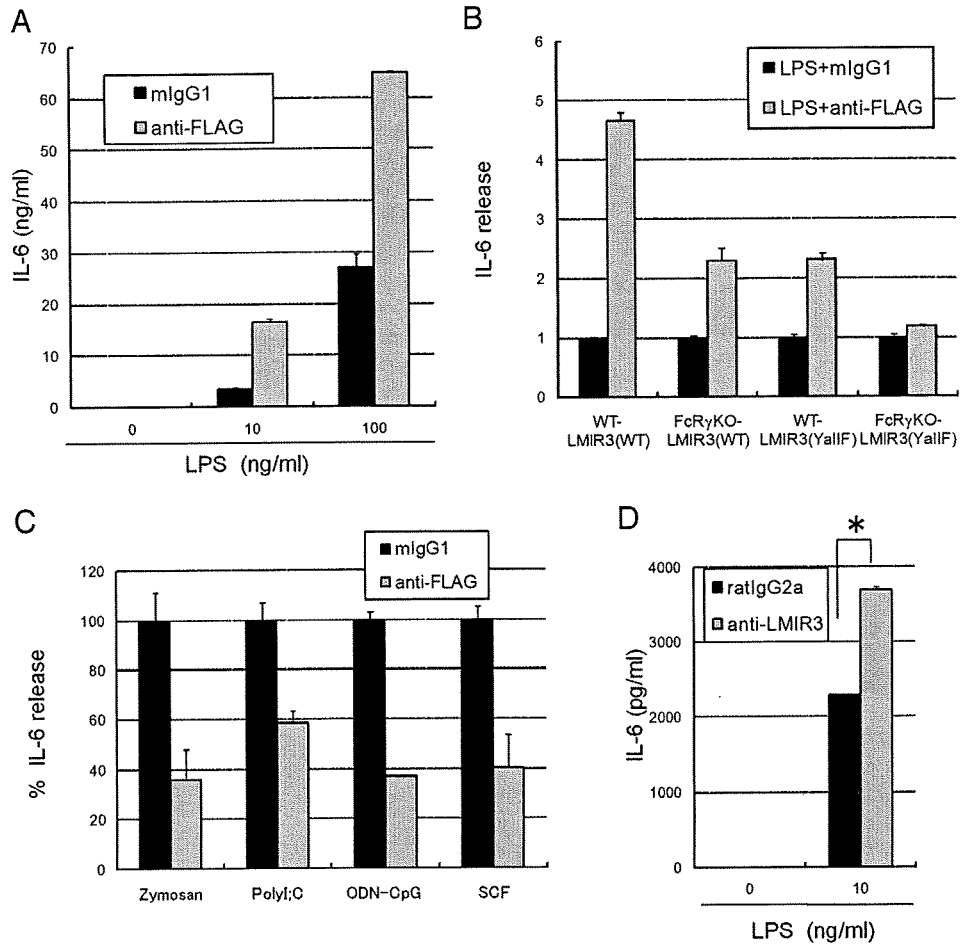

FIGURE 6. LMIR3 crosslinking enhances cytokine production of BMMCs stimulated by LPS, while suppressing that stimulated by zymosan, poly(I:C), CpG0ODN, or SCF. *A*, BMMCs transduced with FLAG-tagged LMIR3(WT) were stimulated by either $F(ab')_2$ anti-FLAG mAb or $F(ab')_2$ mouse IgG1 mAb together with 0, 10, or 1000 ng/ml LPS. IL-6 released into the culture supernatants was measured by ELISA. All data points correspond to the mean and the SD of four independent experiments. *B*, The ratio of the amounts of IL-6 released by each transfectant in response to $F(ab')_2$ anti-FLAG mAb and 10 ng/ml LPS to those in response to $F(ab')_2$ mouse IgG1 as control and 10 ng/ml LPS. WT or FcRγ-deficient BMMCs were transduced with FLAG-tagged LMIR3(WT) or (YallF). IL-6 released into the culture supernatants was measured by ELISA. All data points correspond to the mean and the SD. One representative of three independent experiments is shown. WT-LMIR3(WT) or WT-LMIR3(YallF) indicates WT BMMCs transduced with FLAG-tagged LMIR3(WT) or LMIR3(YallF) mutant, respectively. FcRγKO-LMIR3(WT) or FcRγKO-LMIR3(YalF) indicates FcRγ-deficient BMMCs transduced with FLAG-tagged LMIR3(WT) or LMIR3(YallF) mutant, respectively. *C*, BMMCs transduced with FLAG-tagged LMIR3(WT) were stimulated by either $F(ab')_2$ anti-FLAG mAb or $F(ab')_2$ mouse IgG1 mAb together with either 100 μg/ml zymosan, 250 μg/ml poly(I:C), 5 μg/ml CpG-ODN, or 100 ng/ml SCF. IL-6 released into the culture supernatants was measured by ELISA. All data points correspond to the mean and the SD of three independent experiments. *D*, BMMCs were stimulated either anti-LMIR3 Ab or rat IgG2a together or not with 10 ng/ml LPS. All data points correspond to the mean and the SD of four independent experiments. *, $p < 0.05$.

stimulated by LPS, a TLR4 ligand (Fig. 6*A*). To delineate the contribution of FcRγ and/or LMIR3 cytoplasmic tyrosine residues to the LMIR3-mediated enhancement of cytokine production of mast cells stimulated by LPS, we utilized either LMIR3(WT) or LMIR3(YallF)-transduced WT or FcRγ-deficient BMMCs. We then measured the ratio of the amount of cytokine production in BMMCs stimulated by LPS plus LMIR3 crosslinking to that in BMMCs stimulated by LPS alone, finding the ratios to be ~4.7 in LMIR3(WT)-transduced WT BMMCs, ~2.2 in LMIR3(WT)-transduced FcRγ-deficient BMMCs, ~2.2 in LMIR3(YallF)-transduced WT BMMCs, or ~1.1 in LMIR3(YallF)-transduced FcRγ-deficient BMMCs. Taken together, these results indicated that both FcRγ and LMIR3 cytoplasmic tyrosine residues played an important role in LMIR3-mediated enhancement of cytokine production of BMMCs stimulated by LPS (Fig. 6*B*). In contrast, LMIR3 crosslinking impaired cytokine production of LMIR3-transduced BMMC stimulated by zymosan, poly(I:C), or CpG-ODN, which are ligands for TLR2, TLR3, or TLR9, respectively, or SCF (Fig. 6*C*). Finally, and most importantly, endogenous LMIR3 crosslinking induced significant levels of enhancement of cytokine production in BMMCs stimulated by LPS (Fig. 6*D*). In summary, LMIR3 functions as an activating receptor in BMMCs stimulated by TLR4 ligand, while LMIR3 functions as an inhibitory receptor in BMMCs stimulated by other TLR agonists or SCF.

Discussion

The biological role of paired immune receptors remains incompletely understood, but recent advances postulate their main functions in innate immunity. Paired activating receptors respond rapidly and effectively to foreign pathogens such as bacteria or viruses, while paired inhibitory receptors suppress the steady-state response to self proteins or excessive inflammation under pathological conditions. Generally, the former associate with ITAM or

ITAM-related activating motif-bearing adaptor molecules to transmit an activating signal, while the latter contain ITIM in the cytoplasmic region to transmit an inhibitory signal (1, 2, 27, 28). On the other hand, growing evidence has recently established the concept of dual functionality of an immune receptor that is related to the concept of inhibitory ITAM or activating ITIM (29–34). In fact, some ITAM-containing receptors can deliver an inhibitory signal in a cell type and stimulation-dependent manner, as exemplified by the inhibitory effect of triggering receptor expressed on myeloid cells 2 (TREM-2) on LPS response (35, 36) or FcαRI on monomeric IgA response (37). Conversely, ITIM-containing receptors transmitting an activating signal are rare, but, for example, platelet-endothelial cell adhesion molecule-1 (PECAM-1) can promote endothelial cell migration (38). Additionally, ITSM-containing receptors, such as SLAM family immunoreceptors, also exhibit dual functionality (23). For instance, 2B4 (CD244)-mediated NK cell activity was promoted or suppressed by the association of its ITSM with SH2D1A or EAT-2, respectively (39).

In the present study, we delineated the dual function of LMIR3 in mast cells. As expected from the structural characteristic that LMIR3 contains two ITIMs in the cytoplasmic region, LMIR3 exerted an inhibitory effect on FcεRI-mediated cytokine production in mast cells. However, analysis of different LMIR3 mutants demonstrated that the maximum inhibitory function as well as the maximum association of LMIR3 with SHP-1 or SHP-2 required an ITSM (including Y5) in addition to two ITIMs (including Y1 and Y3) (Fig. 2*E*). Remarkably, both Y1 and Y5 (Y1/5) played a predominant role (Y1/5 > Y3/5 > Y1/3) in the association of LMIR3 with SHP-1 or SHP-2, while a single tyrosine residue (Y1, Y3, or Y5) had a minimum role. These results strongly suggested an indispensable role of ITSM and the differential roles of two ITIMs in the inhibitory function of LMIR3. However, adaptor molecules with positive functions to associate with LMIR3 via its ITSM might be able to interfere with the inhibitory function of LMIR3. Additionally, how SHP-1 and SHP-2 differentially contribute to LMIR3-mediated inhibition in mast cells remains to be resolved.

On the other hand, the potential of ITIM-containing LMIR3 to function as an activating receptor was illustrated by experimental results that in mast cells, crosslinking of LMIR3(Y1/3/5F) mutant lacking the inhibitory function induced high amounts of cytokine production (Fig. 4*A*) as well as the activation of ERK and Akt (Fig. 5*C*) and the association of p85 with phosphorylated LMIR3(Y1/3/5F) (Fig. 4*D*). In support of this, LMIR3 associated with p85 exclusively via phosphorylated Y2 (Fig. 3*B*). Therefore, it is anticipated that PI3K will be important to the LMIR3-mediated activating pathway. Additionally, the association of LMIR3 with Grb2 was also recognized (Fig. 3*A*), but LMIR3 tyrosine residues responsible for the binding could not be identified (data not shown) notwithstanding the fact that Y4 is located in the binding motif for Grb2. This might be either because Grb2 is not easy to discriminate from Ig L chain in coimmunoprecipitation experiments or because LMIR3 associates with Grb2 but not necessarily via Y4. Further examination is necessary, but the association of LMIR3 with Grb2 should lead to the activation of Ras/ERK in the LMIR3-mediated activating pathway. Indeed, these results do not always conflict with recent reports on IREM-1/human LMIR3, but there exists the striking difference between mouse and human LMIR3. Unlike IREM-1, crosslinking of LMIR3(YallF), in which all cytoplasmic tyrosine residues were replaced with phenylalanine, still induced significant levels of cytokine production in mast cells. We then asked if there exists an LMIR3-mediated activating signaling pathway independent of LMIR3 cytoplasmic tyrosine residues, and concluded that LMIR3 associates with ITAM-bearing FcRγ, thereby transmitting an activating signal in mast cells independently of tyrosines. Since LMIR3 contains no charged residues in the transmembrane domain, the association of LMIR3 with FcRγ appears not to be through pairwise interaction of basic and acidic residues. Related to this, surface expression levels of LMIR3, unlike typical activating receptors associating with FcRγ, were not affected by FcRγ deficiency. Simultaneously, we also found that cytokine production induced by triggering LMIR3(Y1/3/5F) or LMIR3(YallF) mutant, with the former being at much higher levels than the latter, was severely or completely, respectively, suppressed by FcRγ deficiency. This suggested that FcRγ played a predominant role as compared with Y2/4 of LMIR3 in LMIR3-mediated cytokine production. With the exception that killer cell Ig-like receptor (KIR)2DL4 contains ITIM in the cytoplasmic domain and a basic transmembrane residue through which it associates with FcRγ, LMIR3 is unusual in that an ITIM-containing receptor associates with an ITAM-bearing adaptor. Intriguingly, KIR2DL4 functions only as an activating receptor despite its bearing ITIM, whereas LMIR3 can function as either an inhibitory receptor via ITIM and ITSM or an activating receptor via Y276/303 and association with FcRγ. Additionally, several differences exist between mouse and human LMIR3. 1) IREM-1 associated with p85 via Y236 and Y263, both of which fit the binding motif for p85, while mouse LMIR3 did so only via Y2 (Fig. 3*B*). 2) Membrane-proximal ITIM played a predominant role in the inhibitory function of IREM-1, whereas ITSM did so in the case of LMIR3 (Figs. 2*E* and 3). 3) IREM-1 associated with SHP-1, but not SHP-2, while LMIR3 associated with both SHP-1 and SHP-2 (Fig. 3). 4) Coligation of IREM-1 and FcεRI in RBL cells induced an inhibition of the release of β-hexosaminidase, a marker of degranulation, while coligation of mouse LMIR3 and FcεRI in BMMCs led to the impairment of cytokine production, but not significant degranulation (Fig. 1 and data not shown). The difference might be explained by the different experimental systems including the quality of Ab used. On the other hand, because degranulation requires stronger FcεRI aggregation than cytokine production in BMMCs, a stronger inhibitory signal may be necessary for the inhibition of degranulation as compared with cytokine production (13, 41, 42). Accordingly, it is possible that mouse LMIR3 has relatively weaker inhibitory activities in comparison to human LMIR3, while having stronger activating activities via FcRγ in mast cells. From this point of view, the potential of mouse, but not human, LMIR3 to associate with SHP-2 might influence the magnitude of the inhibitory signal.

Most importantly, we found physiological conditions under which LMIR3 functions as an activating receptor in mast cells. As clearly demonstrated in Fig. 6, cytokine production of mast cells stimulated by LPS was profoundly enhanced by LMIR3 engagement, where the activating effect of LMIR3 on TLR4 signaling was dependent on FcRγ and LMIR3 cytoplasmic tyrosine residues. Considering that TLR4 expressed in mast cells plays a critical protective role in a model of acute septic peritonitis (43–45), LMIR3 signaling may either protect against enterobacterial infection or, conversely, cause prolonged excessive inflammation by enhancing the TLR4 signal. On the other hand, cytokine production of mast cells stimulated by SCF or other TLR agonists such as zymosan, poly(I:C), or CpG-ODN was impaired by LMIR3 crosslinking, although these stimuli did not affect surface expression levels of LMIR3 in mast cells (Fig. 6 and data not shown). Interestingly, these inhibitory events did not require coengagement of LMIR3 and TLRs or c-kit, whereas the inhibition of FcεRI signaling required coengagement of LMIR3 and FcεRI. In fact, the inhibition was not significantly observed when FcεRI and LMIR3 were engaged by anti-TNP IgE plus TNP-BSA and anti-LMIR3

Ab, respectively; that is, FcεRI and LMIR3 were separately engaged (data not shown). Collectively, the quality and quantity of stimuli may determine the function of LMIR3 as well as the phosphorylation levels of each LMIR3 tyrosine residue. The generation of Ab specific for each phosphorylated tyrosine of LMIR3 will give a clue to the stimulation-dependent LMIR3 function. To clarify the precise mechanism under which LMIR3 functions as an activating or inhibitory receptor is an important issue. Whether LMIR3 associates with TLR, where LMIR3- and TLR-mediated signaling pathways are combined, and how the quality and quantity of stimuli modulate the function of LMIR3 are all questions that remain to be resolved. In any case, LMIR3 can positively or negatively regulate TLR responses in mast cells, strongly suggesting the involvement of LMIR3 in the modulation of innate immunity. In view of the regulation of an activating and inhibitory signal in the immune system, the dual functionality of LMIR3 and its relevant mechanism presented here is unique and intriguing. Based on the counterbalance theory for evolution and function of paired receptors (46), we could hypothesize an in vivo function of LMIR3 as follows: if any pathogen utilized an inhibitory receptor LMIR3 to down-regulate responses against itself, another activating LMIR might have evolved to interact with it and thereby act as a counterbalance. Simultaneously, LMIR3 also might have evolutionally acquired the activating function to enhance TLR4 signal. Under normal conditions, LMIR3 constitutively inhibits weak signals in the steady-state from cytokine/chemokine or self-Ag through binding to an unknown endogenous ligand. Consequently, appropriate myeloid cell differentiation, distribution, and activation will be maintained, and the occurrence of autoimmune diseases will be avoided. Although both identification of a ligand for LMIR3 and analysis of LMIR3-deficient mice are indispensable to fully understand the function of LMIR3, this study will lead to the delineation of a novel aspect of immune regulation.

In conclusion, this study provides the first demonstration that an inhibitory receptor LMIR3 associates with FcRγ and thereby enhances LPS response in mast cells. Dual functions of LMIR3 are expected to play an important part in maintaining homeostasis and in responding to emergencies in immunity.

Acknowledgments

We thank Dr. Hisashi Arase for providing pME18S expression vector containing a mouse CD150 leader segment (43). We are grateful to Dr. Dovie Wylie for her excellent language assistance.

Disclosures

Toshio Kitamura serves as a consultant for R&D Systems.

References

1. Ravetch, J. V., and L. L. Lanier. 2000. Immune inhibitory receptors. *Science* 290: 84–89.
2. Takai, T., and M. Ono. 2001. Activating and inhibitory nature of the murine paired immunoglobulin-like receptor family. *Immunol. Rev.* 181: 215–222.
3. Kumagai, H., T. Oki, K. Tamitsu, S. Z. Feng, M. Ono, H. Nakajima, Y. C. Bao, Y. Kawakami, K. Nagayoshi, N. G. Copeland, et al. 2003. Identification and characterization of a new pair of immunoglobulin-like receptors LMIR1 and 2 derived from murine bone marrow-derived mast cells. *Biochem. Biophys. Res. Commun.* 307: 719–729.
4. Izawa, K., J. Kitaura, Y. Yamanishi, T. Matsuoka, T. Oki, F. Shibata, H. Kumagai, H. Nakajima, M. Maeda-Yamamoto, J. P. Hauchins, et al. 2007. Functional analysis of an activating receptor LMIR4 as a counterpart of an inhibitory receptor LMIR3. *J. Biol. Chem.* 282: 17997–18008.
5. Yamanishi, Y., J. Kitaura, K. Izawa, T. Matsuoka, T. Oki, Y. Lu, F. Shibata, S. Yamazaki, H. Kumagai, H. Nakajima, et al. 2008. Analysis of mouse LMIR5/CLM-7 as an activating recptor: differential regulation of LMIR5/CLM-7 in mouse versus human cells. *Blood* 111: 688–698.
6. Chung, D. H., M. B. Humphrey, M. C. Nakamura, D. G. Ginzinger, W. E. Seaman, and M. R. Daws. 2003. CMRF-35-like molecule-1, a novel mouse myeloid receptor, can inhibit osteoclast formation. *J. Immunol.* 171: 6541–6548.
7. Yotsumoto, K., Y. Okoshi, K. Shibuya, S. Yamazaki, S. Tahara-Hanaoka, S. Honda, M. Osawa, A. Kuroiwa, Y. Matsuda, D. G. Tenen, et al. 2003. Paired activating and inhibitory immunoglobulin-like receptors, MAIR-I and MAIR-II, regulate mast cell and macrophage activation. *J. Exp. Med.* 198: 223–233.
8. Luo, K., W. Zhang, L. Sui, N. Li, M. Zhang, X. Ma, L. Zhang, and X. Cao. 2001. DIgR1, a novel membrane receptor of the immunoglobulin gene superfamily, is preferentially expressed by antigen-presenting cells. *Biochem. Biophys. Res. Commun.* 287: 35–41.
9. Daish, A., G. C. Starling, J. L. McKenzie, J. C. Nimmo, D. G. Jackson, and D. N. Hart. 1993. Expression of the CMRF-35 antigen, a new member of the immunoglobulin gene superfamily, is differentially regulated on leukocytes. *Immunology* 79: 55–63.
10. Can, I., S. Tahara-Hanaoka, K. Hitomi, T. Nakano, C. Nakahashi-Oda, N. Kurita, S. Honda, K. Shibuya, and A. Shibuya. 2008. Caspase-independent cell death by CD300LF (MAIR-V), an inhibitory immunoglobulin-like receptor on myeloid cells. *J. Immunol.* 180: 207–213.
11. Shi, L., K. Luo, D. Xia, T. Chen, G. Chen, Y. Jiang, N. Li, and X. Cao. 2006. DIgR2, dendritic cell-derived immunoglobulin receptor 2, is one representative of a family of IgSF inhibitory receptors and mediates negative regulation of dendritic cell-initiated antigen-specific T-cell responses. *Blood* 108: 2678–2686.
12. Fujimoto, M., H. Takatsu, and H. Ohno. 2006. CMRF-35-like molecule-5 constitutes novel paired receptors, with CMRF-35-like molecule-1, to transduce activation signal upon association with FcRγ. *Int. Immunol.* 18: 1499–1508.
13. Kawakami, T., and S. J. Galli. 2002. Regulation of mast cell and basophil function and survival. *Nat. Rev. Immunol.* 2: 773–786.
14. Galli, S. J., S. Nakae, and M. Tsai. 2005. Mast cells in the development of adaptive immune responses. *Nat. Immunol.* 6: 135–142.
15. Kraft, S., and J. P. Kinet. 2007. New developments in FcεRI regulation, function and inhibition. *Nat. Rev. Immunol.* 7: 365–378.
16. Daëron, M., S. Latour, O. Malbec, E. Espinosa, P Pina, S. Pasmans, and W. H. Fridman. 1995. The same tyrosine-based inhibition motif, in the intracytoplasmic domain of FcγRIIB, regulates negatively BCR-, TCR-, and FcR-dependent cell activation. *Immunity* 3: 635–646.
17. Katz, H. R., E. Vivier, M. C. Castells, M. J. McCormick, J. M. Chambers, and K. F. Austen. 1996. Mouse mast cell gp49B1 contains two immunoreceptor tyrosine-based inhibition motifs and suppresses mast cell activation when coligated with the high-affinity Fc receptor for IgE. *Proc. Natl. Acad. Sci. USA* 93: 10809–10814.
18. Uehara, T., M. Bléry, D. W. Kang, C. C. Chen, L. H. Ho, G. L. Gartland, F. T. Liu, E. Vivier, M. D. Cooper, and H. Kubagawa. 2001. Inhibition of IgE-mediated mast cell activation by the paired Ig-like receptor PIR-B. *J. Clin. Invest.* 108: 1041–1050.
19. Yamashita, Y., M. Ono, and T. Takai. 1998. Inhibitory and stimulatory functions of paired Ig-like receptor (PIR) family in RBL-2H3 cells. *J. Immunol.* 161: 4042–4047.
20. Bachelet, I., A. Munitz, A. Moretta, L. Moretta, and F. Levi-Schaffer. 2005. The inhibitory receptor IRp60 (CD300a) is expressed and functional on human mast cells. *J. Immunol.* 175: 7989–7895.
21. Okoshi, Y., S. Tahara-Hanaoka, C. Nakahashi, S. Honda, A. Miyamoto, H. Kojima, T. Nagasawa, K. Shibuya, and A. Shibuya. 2005. Requirement of the tyrosines at residues 258 and 270 of MAIR-I in inhibitory effect on degranulation from basophilic leukemia RBL-2H3. *Int. Immunol.* 17: 65–72.
22. Sidorenko, S. P., and E. A. Clark. 2003. The dual-function CD150 receptor subfamily: the viral attraction. *Nat. Immunol.* 4: 19–24.
23. Chemnitz, J. M., R. V. Parry, K. E. Nichols, C. H. June, and J. L. Riley. 2004. SHP-1 and SHP-2 associate with immunoreceptor tyrosine-based switch motif of programmed death 1 upon primary human T cell stimulation, but only receptor ligation prevents T cell activation. *J. Immunol.* 173: 945–954.
24. Alvarez-Errico, D., H. Aguilar, F. Kitzig, T. Brckalo, J. Sayós, and M. López-Botet. 2004. IREM-1 is a novel inhibitory receptor expressed by myeloid cells. *Eur. J. Immunol.* 34: 3690–3701.
25. Alvarez-Errico, D., J. Sayós, and M. López-Botet. 2007. The IREM-1 (CD300f) inhibitory receptor associates with the p85α subunit of phosphoinositide 3-kinase. *J. Immunol.* 178: 808–816.
26. Takai, T., M. Li, D. Sylvestre, R. Clynes, and J. V. Ravetch. 1994. FcR γ chain deletion results in pleiotrophic effector cell defects. *Cell* 76: 519–529.
27. Colonna, M. 2003. TREMs in the immune system and beyond. *Nat. Rev. Immunol.* 3: 445–453.
28. Humphrey, M. B., L. L. Lanier, and M. C. Nakamura. 2005. Role of ITAM-containing adapter proteins and their receptors in the immune system and bone. *Immunol. Rev.* 208: 50–65.
29. Underhill, D. M., and H. S. Goodridge. 2007. The many faces of ITAMs. *Treands Immunol.* 28: 66–73.
30. Pinheiro da Silva, F., M. Aloulou, M. Benhamou, and R. C. Monteiro. 2008. Inhibitory ITAMs: a matter of life and death. *Trends Immunol.* 29: 366–373.
31. Hamerman, J. A., N. K. Tchao, C. A. Lowell, and L. L. Lanier. 2005. Enhanced Toll-like receptor responses in the absence of signaling adaptor DAP12. *Nat. Immunol.* 6: 579–586.
32. Turnbull, I. R., J. E. McDunn, T. Takai, R. R. Townsend, J. P. Cobb, and M. Colonna. 2005. DAP12 (KARAP) amplifies inflammation and increases mortality from endotoxemia and septic peritonitis. *J. Exp. Med.* 202: 363–369.
33. Takaki, R., S. R. Watson, and L. L. Lanier. 2006. DAP12: an adapter protein with dual functionality. *Immunol. Rev.* 214: 118–129.
34. Turnbull, I. R., and M. Colonna. 2007. Activating and inhibitory functions of DAP12. *Nat. Rev. Immunol.* 7: 155–161.
35. Hamerman, J. A., J. R. Jarjoura, M. B. Humphrey, M. C. Nakamura, W. E. Seaman, and L. L. Lanier. 2006. Cutting edge: inhibition of TLR and FcR responses in macrophages by triggering receptor expressed on myeloid cells (TREM)-2 and DAP12. *J. Immunol.* 177: 2051–2055.

36. Turnbull, I. R., S. Gilfillan, M. Cella, T. Aoshi, M. Miller, L. Piccio, M. Hernandez, and M. Colonna. 2006. Cutting edge: TREM-2 attenuates macrophage activation. *J. Immunol.* 177: 3520–3254.
37. Pasquier, B., P. Launay, Y. Kanamaru, I. C. Moura, S. Pfirsch, C. Ruffié, D. Hénin, M. Benhamou, M. Pretolani, U. Blank, et al. 2005. Identification of FcαRI as an inhibitory receptor that controls inflammation: dual role of FcRγ ITAM. *Immunity* 22: 31–42.
38. Wee, J. L., and D. E. Jackson. 2005. The Ig-ITIM superfamily member PECAM-1 regulates the "outside-in" signaling properties of integrin $\alpha_{IIb}\beta_3$ in platelets. *Blood* 106: 3816–3823.
39. Roncagalli, R., J. E. Taylor, S. Zhang, X. Shi, R. Chen, M. E. Cruz-Munoz, L. Yin, S. Latour, and A. Veillette. 2005. Negative regulation of natural killer cell function by EAT-2, a SAP-related adaptor. *Nat. Immunol.* 10: 1002–1010.
40. Kikuchi-Maki, A., S. Yusa, T. L. Catina, and K. S. Campbell. 2003. KIR2DL4 is an IL-2-regulated NK cell receptor that exhibits limited expression in humans but triggers strong IFN-γ production. *J. Immunol.* 171: 3415–3425.
41. Kitaura, J., J. Song, M. Tsai, K. Asai, M. Maeda-Yamamoto, A. Mocsai, Y. Kawakami, F. L. Liu, C. A. Lowell, B. G. Barisas, et al. 2003. Evidence that IgE molecules mediate a spectrum of effects on mast cell survival and activation via aggregation of the FcεRI. *Proc. Natl. Acad. Sci. USA* 100: 12911–12916.
42. Kawakami, T., and J. Kitaura. 2005. Mast cell survival and activation by IgE in the absence of antigen: a consideration of the biologic mechanisms and relevance. *J. Immunol.* 175: 4167–4173.
43. Supajatura, V., H. Ushio, A. Nakao, K. Okumura, C. Ra, and H. Ogawa. 2001. Protective roles of mast cells against enterobacterial infection are mediated by Toll-like receptor 4. *J. Immunol.* 167: 2250–2256.
44. Malaviya, R., T. Ikeda, E. Ross, and S. N. Abraham. 1996. Mast cell modulation of neutrophil influx and bacterial clearance at sites of infection through TNF-α. *Nature* 381: 77–80.
45. Echtenacher, B., D. N. Mannel, and L. Hultner. 1996. Critical protective role of mast cells in a model of acute septic peritonitis. *Nature* 381: 75–77.
46. Barclay, A. N., and D. Hatherley. 2008. The counterbalance theory for evolution and function of paired receptors. *Immunity* 29: 675–678.

MOLECULAR AND CELLULAR BIOLOGY, Apr. 2009, p. 1796–1813 Vol. 29, No. 7
0270-7306/09/$08.00+0 doi:10.1128/MCB.01423-08

A Rac GTPase-Activating Protein, MgcRacGAP, Is a Nuclear Localizing Signal-Containing Nuclear Chaperone in the Activation of STAT Transcription Factors▽†

Toshiyuki Kawashima,[1]‡* Ying Chun Bao,[1]‡ Yukinori Minoshima,[1] Yasushi Nomura,[1] Tomonori Hatori,[1] Tetsuya Hori,[2] Tatsuo Fukagawa,[2] Toshiyuki Fukada,[3,4] Noriko Takahashi,[1] Tetsuya Nosaka,[1,5] Makoto Inoue,[6] Tomohiro Sato,[6,7] Mutsuko Kukimoto-Niino,[6] Mikako Shirouzu,[6] Shigeyuki Yokoyama,[6,7] and Toshio Kitamura[1]*

Division of Cellular Therapy, Institute of Medical Science, University of Tokyo, Minato-ku, Tokyo 108-8639, Japan[1]; Department of Molecular Genetics, National Institute of Genetics and the Graduate University for Advanced Studies, Mishima, Shizuoka 411-8540, Japan[2]; Laboratory for Cytokine Signaling, RIKEN Research Center for Allergy and Immunology,[3] and Protein Research Group, Genomic Sciences Center, Yokohama Institute, RIKEN,[6] 1-7-22 Suehiro-cho, Tsurumi, Yokohama 230-0045, Japan; Department of Allergy and Immunology, Osaka University Graduate School of Medicine, Osaka University, 2-2 Yamada-oka, Suita, Osaka 565-0871, Japan[4]; Department of Microbiology, Mie University Graduate School of Medicine, 2-174 Edobashi, Tsu 514-8507, Japan[5]; and Department of Biophysics and Biochemistry, Graduate School of Science, University of Tokyo, 7-3-1 Hongo, Bunkyo-ku, Tokyo 113-0033, Japan[7]

Received 10 September 2008/Returned for modification 1 November 2008/Accepted 12 January 2009

In addition to their pleiotropic functions under physiological conditions, transcription factors STAT3 and STAT5 also have oncogenic activities, but how activated STATs are transported to the nucleus has not been fully understood. Here we show that an MgcRacGAP mutant lacking its nuclear localizing signal (NLS) blocks nuclear translocation of p-STATs both in vitro and in vivo. Unlike wild-type MgcRacGAP, this mutant did not promote complex formation of phosphorylated STATs (p-STATs) with importin α in the presence of GTP-bound Rac1, suggesting that MgcRacGAP functions as an NLS-containing nuclear chaperone. We also demonstrate that mutants of STATs lacking the MgcRacGAP binding site (the strand βb) are hardly tyrosine phosphorylated after cytokine stimulation. Intriguingly, mutants harboring small deletions in the C′-adjacent region (βb-βc loop region) of the strand βb became constitutively active with the enhanced binding to MgcRacGAP. The molecular basis of this phenomenon will be discussed, based on the computer-assisted tertiary structure models of STAT3. Thus, MgcRacGAP functions as both a critical mediator of STAT's tyrosine phosphorylation and an NLS-containing nuclear chaperone of p-STATs.

The STAT (signal transducers and activators of transcription) family proteins (STAT1 to -4, -5A, -5B, and -6) are phosphorylated by cytokine stimulation, form homo- or heterodimers, and enter the nucleus, where they regulate expression of their target genes (6, 13). STATs have a variety of functions, including antiapoptosis, proliferation, differentiation, inflammation, and development under physiological conditions, and of note, the oncogenic activities of STAT3 and STAT5 have also been demonstrated under pathological conditions (5).

A small GTPase Rac1 is implicated in cytoskeletal organization, membrane ruffling, production of superoxide, phagocytosis, and chemotaxis as well as regulation of the cell cycle (15, 39). Recent studies revealed its distinct roles in nuclear translocation of phosphorylated STATs (p-STATs) and β-catenin and also its nuclear accumulation in the G_2 phase, promoting cell division (17, 31, 47). MgcRacGAP is an evolutionarily conserved GTPase-activating protein (GAP) for Rho family GTPases. We and others previously showed that MgcRacGAP controls the mitotic spindle through associating α-, β-, and γ-tubulin, Rho family GTPases, and a kinesin protein, MKLP1, and plays essential roles in the completion of cytokinesis, accumulating to the midbody (12, 16, 32). Very recently, Yamada et al. reported that conditional knockout of MgcRacGAP results in acute apoptosis even before the failure of cytokinesis in interleukin-7 (IL-7)-expanded $B220^+$ cells (48), indicating that MgcRacGAP is not simply involved in cell division but also in cell survival, at least in IL-7-expanded $B220^+$ cells.

Molecular trafficking between the nucleus and cytoplasm occurs via nuclear pore complexes. To enter the nucleus, nuclear proteins larger than ~50 kDa usually harbor a functional nuclear localization signal (NLS) or bind NLS-containing chaperones. The best-characterized NLS is the mono- or bipartite polybasic NLS. Polybasic NLS-containing proteins are usually recognized by importin α/β heterodimers, importin β docks the ternary complex to the nuclear pore, and the complex migrates into the nucleus. Then, the GTP-bound form of small GTPase Ran directly binds to importin β in the complex,

* Corresponding author. Mailing address: Division of Cellular Therapy, Institute of Medical Science, University of Tokyo, Minato-ku, Tokyo 108-8639, Japan. Phone: 81-3-5449-5758. Fax: 81-3-5449-5453. E-mail for Toshiyuki Kawashima: kkawa@ims.u-tokyo.ac.jp. E-mail for Toshio Kitamura: kitamura@ims.u-tokyo.ac.jp.

† Supplemental material for this article may be found at http://mcb.asm.org/.

‡ T.K. and Y.C.B. contributed equally to this work.

▽ Published ahead of print on 21 January 2009.

followed by disassembly of the complex inside the nucleus (11, 29). In addition to the polybasic NLS proline, tyrosine-containing NLSs (PY-NLSs) have been reported to be a different class of NLS; these NLSs mediate direct binding of NLS-containing proteins to karyopherin β2 (24).

How activated STATs are transported to the nucleus has been investigated; activated STAT1 and STAT3 were reported to bind importin α5 and several importin αs, respectively, which mediated the nuclear transport of STATs (25, 26, 30, 42, 44). Molecules other than importins and Ran also participate in the regulation of the nuclear translocation of STATs (27). We recently found that GTP-bound Rac1 and MgcRacGAP form a ternary complex with p-STATs and play critical roles in the nuclear translocation of p-STATs via the importin α/β pathway in an in vitro nuclear transport assay (17). However, it remained elusive how GTP-bound Rac1 and MgcRacGAP mediate the complex formation of p-STATs with importin αs. Moreover, the regulation of nuclear import of activated STATs by MgcRacGAP has not been fully demonstrated in vivo, because MgcRacGAP also plays an essential role in the completion of cytokinesis (12, 16, 33, 45). Therefore, the phenotypes observed in MgcRacGAP-depleted cells may include the effects of cytokinesis failure.

In the present work, we demonstrate that the NLS of MgcRacGAP plays essential roles in the nuclear import of p-STATs not only in vitro but also in vivo, by using MgcRacGAP conditional knockout DT40 cells expressing MgcRacGAP mutants lacking the NLS. We also found that the STAT mutants that did not bind MgcRacGAP were hardly phosphorylated on their tyrosine residues by cytokine stimulation, while the STAT mutants that preferentially bound MgcRacGAP exerted strong transcriptional activities even without cytokine stimulation. Thus, MgcRacGAP accompanied by GTP-bound Rac1 is not only an NLS-containing nuclear chaperone of p-STATs but also a critical activator of STAT proteins.

MATERIALS AND METHODS

Purification of recombinant proteins in Sf-9 cells. Purification of recombinant proteins using Sf-9 cells was done as described previously (17). To confirm the purity, the eluted proteins were subjected to sodium dodecyl sulfate-polyacrylamide gel electrophoresis (SDS-PAGE), followed by Coomassie blue (CBB) staining or by Western blotting. Purified His-tagged L69Ran and His-tagged N24Ran were purchased from Cytoskeleton, Inc.

Import assays with permeabilized cells. HeLa cells were grown on poly(L-lysine)-coated coverslips and permeabilized with 40 μg/ml digitonin (Roche) in transport buffer (TB; 20 mM HEPES, pH 7.3, 110 mM KO-acetate, 2 mM $Mg(O\text{-acetate})_2$, 1 mM EGTA, 2 mM dithiothreitol, 0.4 mM phenylmethylsulfonyl fluoride, 3 μg/ml of aprotinin, 2 μg/ml of pepstatin A, 1 μg/ml of leupeptin, 20 mg/ml of bovine serum albumin) for 10 min at room temperature. Subsequently, the cells were washed twice in TB to wash out cytoplasmic proteins. Incubation with 50 μl import mix (IM) was performed at 37°C for 30 min. The IM contained TB, an energy-regenerating system (ERS; 0.5 mM ATP, 0.5 mM GTP, 10 mM creatine phosphate, 30 U/ml creatine phosphokinase) and combinations of 1 μM of the purified proteins indicated in Fig. 2B, below (see also Fig. S2 and S3 in the supplemental material). Following the import reaction, the cells were washed with ice-cold TB and immunostained.

Immunostaining and antibodies. HeLa cells were immunostained as described previously (12). Rabbit anti-STAT5A, anti-STAT3, antihemagglutinin, anti-NF-κB p65, goat anti-glutathione *S*-transferase (anti-GST) (Santa Cruz), mouse anti-Flag (M2; Sigma), rabbit anti-Flag (Zymed), and affinity-purified rabbit anti-MgcRasGAP (12) antibodies (Abs) were used for the first Ab. For the secondary Ab and DNA staining, fluorescein isothiocyanate- or rhodamine-conjugated goat anti-rabbit immunoglobulin (Ig; Wako), fluorescein isothiocyanate- or rhodamine-conjugated goat anti-mouse Ig (Sigma), or rhodamine-conjugated anti-goat Ig (Wako) and 4′,6-diamino-2-phenylindole (DAPI) were used.

Microscopy. Fixed fluorescence images were analyzed on a confocal microscope (FLUOVIEW FV300 scanning laser biological microscope IX70 system; Olympus). Living cells expressing green fluorescent protein (GFP)-fusion proteins were viewed with a fluorescence microscope IX70 (Olympus) equipped with a SenSys/OL cold charge-coupled-device camera (Olympus).

In vitro binding assay, immunoprecipitation, and Western blotting. Immunoprecipitation, gel electrophoresis, and immunoblotting were done as described previously (17), with minor modifications. Purified proteins which were preincubated in the TB with 0.5% Triton X in the in vitro binding assay or cell lysates (2×10^7 cells/ml) were incubated at 4°C for 2 h with the indicated antibodies and protein A-Sepharose. The immunoprecipitates were subjected to Western blot analysis with an anti-tyrosine-phosphorylated STAT5 monoclonal Ab (anti-p-STAT5; Upstate), anti-MgcRacGAP (12), anti-importin β1 (Transduction Laboratories), or anti-MKLP-1, anti-STAT5A, anti-Rac1, or anti-importin α1 (Santa Cruz) antibodies. The filter-bound Ab were detected using the enhanced chemiluminescence system (Amersham). Cytosol and nuclear fractions were prepared, as described previously (17). Fractionation was confirmed by Western blotting with the anti-histone deacetylase (HDAC; for the nuclear fraction) or RhoA (for the cytosol fraction) Ab (Santa Cruz).

Generation of MgcRacGAP conditional knockout cells (5C cells) using DT40 cells. Full-length MgcRacGAP cDNA was cloned into the EcoRI/BamHI site of pUHD10-3 to yield a tetracycline (TET)-sensitive expression plasmid, pUHD-MgcRacGAP. For targeting constructs, a histidinol (hisD) or puromycin (puro) resistance cassette under the control of the β-actin promoter was inserted between the two arms. The targeting constructs and pUHD-MgcRacGAP were transfected into DT40 cells with a GenePulser II electroporator (Bio-Rad). DT40 cells were cultured and transfected as described previously (32). All DT40 cells were cultured at 38°C in Dulbecco's modified medium supplemented with 10% fetal calf serum, 1% chicken serum, penicillin, and streptomycin. To suppress expression of the tetracycline-responsive transgenes, TET (Sigma) was added to the culture medium at a final concentration of 2 μg/ml.

Expression constructs. Flag-tagged wild-type (WT) and mutant MgcRacGAP or STATs were cloned into EcoRI and NotI sites of a mammalian expression vector, pME 18S, or a retrovirus expression vector, pMXs-IG and pMXs-neo. The deletion constructs of MgcRacGAP that lack the internal (INT) domain or various regions of the INT domain were generated by overlapping extension using PCR as described in reference 18. Synthesized oligonucleotides encoding the NLS of MgcRacGAP (NLS-MgcRacGAP; amino acids [aa] 182 to 200), mutant NLS of MgcRacGAP (NLS-MgcRacGAP-182AAA/199AA), or the large T antigen-NLS (PKKKRKV) were cloned into EcoRI and NotI sites of a pMXs-GFP-fusion vector. Site-directed mutagenesis of MgcRacGAP or STATs was done using QuikChange (Stratagene) and the oligonucleotide primers. Several alanine substitution mutants were generated by overlapping extension using PCR. The sequence generated by PCR was confirmed by automated sequencing using an ABI Prism 310 genetic analyzer (Perkin-Elmer).

Production of retroviruses. High-titer retroviruses harboring Cre-recombinase were produced in transient retrovirus packaging cell line PLAT-E or PLAT-A (36).

Cell culture and transfection. The 293T cells were grown in Dulbecco's modified Eagle medium supplemented with 5% fetal calf serum and were transiently transfected with plasmids encoding the wild-type or the mutant forms of STATs using Lipofectamine Plus (Gibco-BRL) according to the manufacturer's recommendations.

Luciferase reporter assay. For the experiments using DT40 cells, pMKIT (mock) or pMKIT/ITD-Flt3 together with 1.0 μg of pME/STAT5A, 1.0 μg of a reporter plasmid carrying a firefly luciferase gene driven by the β-casein promoter, and 0.5 μg of an internal control reporter plasmid with the Rous sarcoma virus long terminal repeat promoter was introduced into 2×10^6 cells of 5C cells with Nucleofector II (Amaxa) set at program B-009 using the Cell Line Nucleofector kit T (Amaxa) according to the manufacturer's instruction. A control vector carrying GFP was introduced to more than 50% of 5C cells under this condition. Sixteen hours after transfection, cells were lysed and were then subjected to a dual luciferase reporter system (Promega). Luciferase activities were also examined in the lysates of 5C transfectants cotransfected with the NF-κB reporter plasmid (k9) carrying a firefly luciferase gene driven by the IL-6 promoter (14) together with an internal control plasmid. After the transfection, cells were incubated with 30 nM phorbol myristate acetate (PMA) and 1 μM ionomycin for 12 h before cell lysates were prepared. For the experiments using 293T cells, cells were transfected with pME (mock) or pME/STAT5As together with 0.5 μg of pME/EPOR, 0.5 μg of a reporter plasmid carrying a firefly luciferase gene driven by the β-casein promoter, and 0.5 μg of an internal control reporter

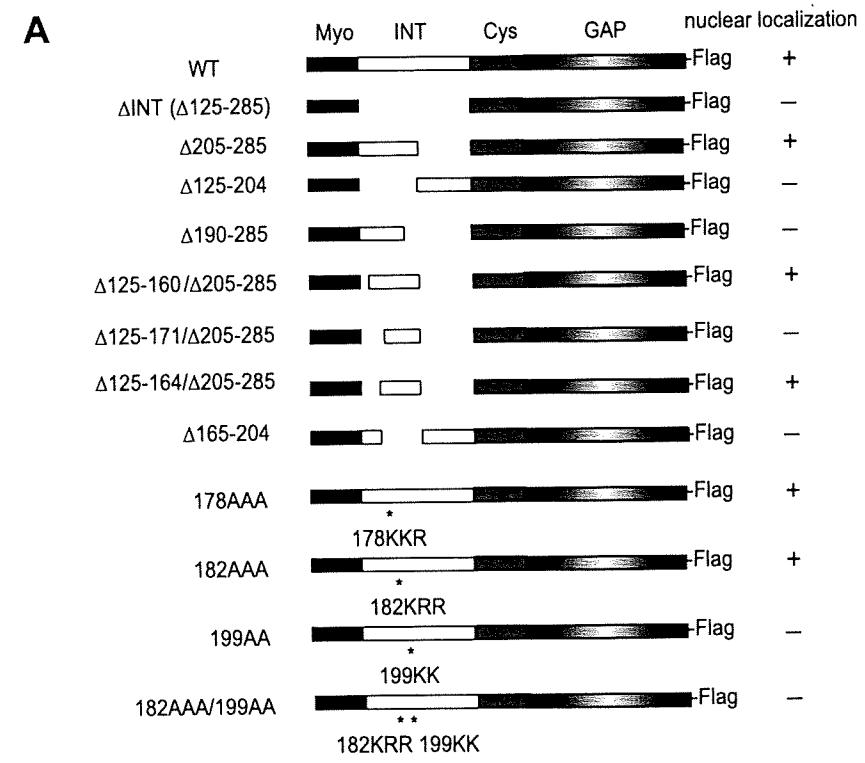
A
Myo
INT
Cys
GAP
nuclear localization
WT
Flag
+
ΔINT (Δ125-285)
Flag
–
Δ205-285
Flag
+
Δ125-204
Flag
–
Δ190-285
Flag
–
Δ125-160/Δ205-285
Flag
+
Δ125-171/Δ205-285
Flag
–
Δ125-164/Δ205-285
Flag
+
Δ165-204
Flag
–
178AAA
Flag
+
178KKR
182AAA
Flag
+
182KRR
199AA
Flag
–
199KK
182AAA/199AA
Flag
–
182KRR 199KK

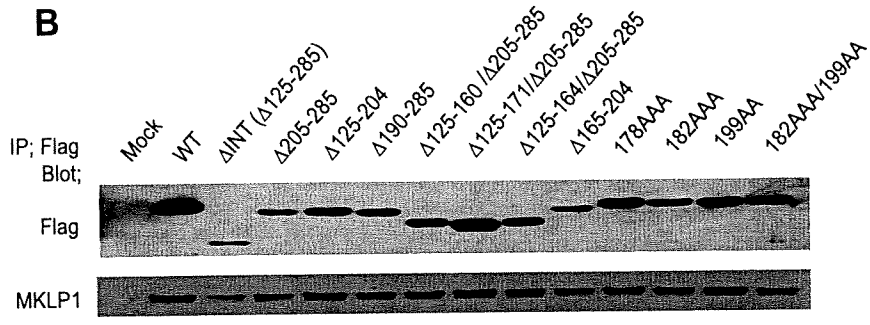
B
IP; Flag
Blot;
Mock
WT
ΔINT (Δ125-285)
Δ205-285
Δ125-204
Δ190-285
Δ125-160 /Δ205-285
Δ125-171/Δ205-285
Δ125-164/Δ205-285
Δ165-204
178AAA
182AAA
199AA
182AAA/199AA
Flag
MKLP1

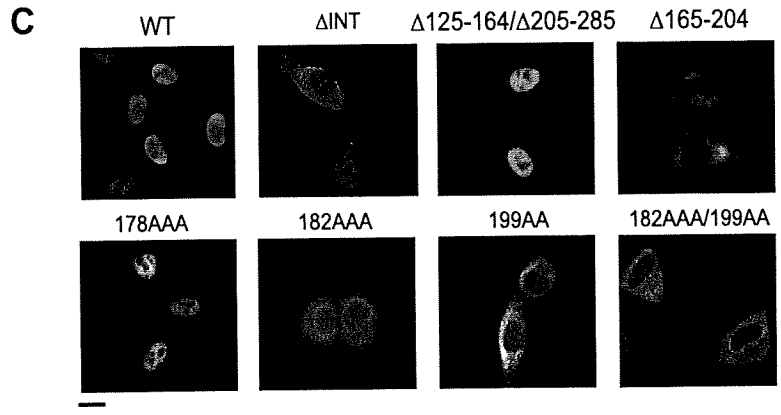
C
WT
ΔINT
Δ125-164/Δ205-285
Δ165-204
178AAA
182AAA
199AA
182AAA/199AA

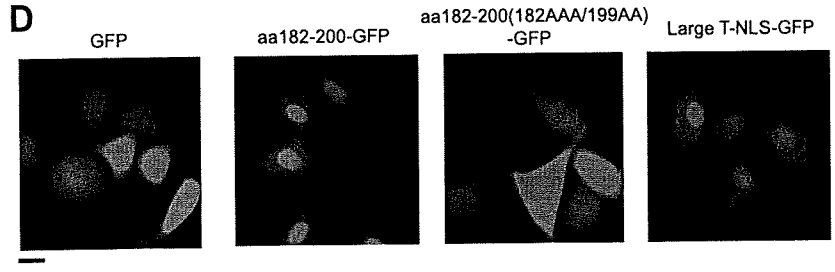
D
GFP
aa182-200-GFP
aa182-200(182AAA/199AA)
-GFP
Large T-NLS-GFP

plasmid with the Rous sarcoma virus long terminal repeat promoter, using Lipofectamine Plus (Gibco-BRL). Twenty-four hours after transfection, cells were stimulated with erythropoietin (EPO; 18 ng/ml; 16 h) and subjected to a dual luciferase reporter system (Promega). To examine the transcriptional activities of STAT3 mutants harboring deletions in DB2, a luciferase assay was done in the lysates of unstimulated or IL-6-stimulated (20 ng/ml) and sIL-6R-stimulated (20 ng/ml) 293T cells cotransfected with the STAT3 reporter plasmid carrying a firefly luciferase gene driven by the mouse glial fibrillary acidic protein promoter (35) together with an internal control reporter plasmid and either the mock vector (pME), the expression vector for the Flag-tagged WT STAT3, or a series of STAT3 mutants harboring deletions in DB2.

Semiquantitative RT-PCR. Gene expression was examined by semiquantitative reverse transcription-PCR (RT-PCR) analysis. One microgram of total RNA was reverse transcribed with random hexamers by using a first-strand cDNA synthesis kit (Pharmacia), and the reaction mixture was subjected to PCR. PCRs were carried out using the following oligonucleotide primers: chicken *Bcl-xL* sense (5′-CGTACCAGAGCTTTGAGCAGGT-3′) and antisense (5′-GACCA AGCACAAGCACAATCAC-3′) and chicken glyceraldehyde-3-phosphate dehydrogenase (*GAPDH*) sense (5′-ATGGTGAAAGTCGGAGTCAACGG-3′) and antisense (5′-ACAGTGCCCTTGAAGTGTCC-3′). PCR was performed under the following conditions to amplify the chicken *Bcl-xL* gene: 96°C for 3 min; 30 cycles of 96°C for 30 s, 63°C for 30 s, and 72°C for 30 s; a final elongation at 72°C for 8 min. To amplify the *GAPDH* gene, conditions were 96°C for 3 min, 20 cycles of 96°C for 30 s, 55°C for 30 s, and 72°C for 30 s, and a final elongation at 72°C for 8 min. Amplification of the product is not saturated at this number of cycles.

Modeling of mutant structures. The models of the D1-10, d356P, d357E, d358L, and L358A mutants of STAT3 were built using the 2.25-Å resolution crystal structure of the STAT3β · DNA complex (2) (PDB ID 1BG1) as a template. Initial models were constructed with the MODELER 9v1 program (9, 28, 41). Then, the models were refined by energy minimization with the AMBER99 force field (46) using MOE computer software (Chemical Computing Group Inc.).

RESULTS

The INT domain of MgcRacGAP contains the bipartite NLS. While endogenous MgcRacGAP localizes both in the cytoplasm and nucleus, overexpressed exogeneous MgcRacGAP mainly accumulates to the nucleus in the interphase in HeLa cells (12). Although MgcRacGAP does not harbor a classic (polybasic) NLS, we found that the ΔINT mutant localized in the cytoplasm (Fig. 1C). These results suggested that the INT domain was critical for the nuclear translocation of MgcRacGAP. To identify a functional NLS of MgcRacGAP, we produced a series of Flag-tagged deletion mutants of the INT domain (Fig. 1A). Protein expression of the mutants and their interaction with a known binding partner, MKLP-1 (34), were confirmed by immunoprecipitation and Western blotting using anti-Flag Ab and anti-MKLP-1 Ab (Fig. 1B). After the immunostaining experiments in HeLa cells, we found that aa 165 to 204 of MgcRacGAP were required for its nuclear localization (Fig. 1C). Since this region contained three polybasic regions (178KKR, 182KRR, and 199KK), we tested whether these polybasic regions could serve as an NLS. We produced alanine substitution mutants (178AAA, 182AAA, 199AA, and 182AAA/199AA) and tested their subcellular localizations. While the 178AAA mutant was located in the nucleus, the 182AAA mutant showed partial cytoplasmic localization, and the 199AA and 182AAA/199AA mutants mostly localized in cytoplasm (Fig. 1C). Next, aa182-200, aa182-200(182AAA/199AA), and a conventional NLS of large T antigen were fused to the N terminus of GFP and we viewed their subcellular localizations with a fluorescence microscope in living cells. As shown in Fig. 1D, aa182-200–GFP and large T-NLS-GFP but not GFP alone or aa182-200(182AAA/199AA)–GFP preferentially accumulated to the nucleus, indicating that aa 182 to 200 is sufficient for a functional polybasic NLS. We also confirmed that leptomycin B treatment, which inhibits nuclear export signal-dependent nuclear export by specific binding to CRM1, did not affect the nuclear or cytoplasmic localization of the WT or 182AAA/199AA mutant, respectively (data not shown). These results suggest that 182KRR and 199KK serve as a functional bipartite NLS for MgcRacGAP. Next, we asked whether MgcRacGAP was transported into the nucleus by importin family members like other proteins carrying NLS. β1Δ450-876, a mutant of importin β1 which lacks the importin α binding site, thereby competitively blocking importin α/β-mediated nuclear import (21), strongly inhibited the nuclear translocation of MgcRacGAP (data not shown). These results implied that MgcRacGAP was transported to the nucleus in an importin α/β-dependent manner.

Importin αs specifically bind MgcRacGAP in yeast through its bipartite NLS. To determine which member of the importin α family is involved in the nuclear transport of MgcRacGAP, we used a yeast two-hybrid system. To test another possibility, that importin β1 directly mediates the nuclear import of MgcRacGAP, we also examined whether importin β1 could directly bind MgcRacGAP. It was found that importin αs specifically bound MgcRacGAP in yeast (see Fig. S1A in the supplemental material). Moreover, purified importin α1 but not importin β1 pulled down MgcRacGAP from HeLa cell lysate (see Fig. S1B in the supplemental material), suggesting that importin α1 but not importin β1 directly bound MgcRacGAP. The purity of isolated importin α1 and importin β1 was confirmed by CBB staining (see Fig. S1C in the supplemental material). To determine if the bipartite NLS of MgcRacGAP indeed mediated its association with importin α1, we tested the interaction of importin α1 with the INT domain, aa 165 to 205, or each of the alanine mutants of MgcRacGAP (182AAA, 199AA, and 182AAA/199AA), and confirmed that the interaction between importin α1 and MgcRacGAP was mediated by the bipartite NLS of MgcRacGAP (see Fig. S1D in the supplemental material). These results demonstrated that MgcRac-

FIG. 1. Identification of the nuclear localization signal of MgcRacGAP. (A) Schematic diagram of various Flag-tagged deletion mutants in the INT domain of MgcRacGAP and summary of the localizations of these mutants. (B) Expression of various deletion mutants and their potential to interact with a known partner, MKLP-1. Cells were transfected with expression vectors carrying Flag-tagged WT or various deletion mutants in the INT domain. After 36 h, cells were immunoprecipitated with the anti-Flag Ab and blotted with the anti-Flag Ab (upper panel) or anti-MKLP-1 Ab (lower panel). (C) Localization of Flag-tagged WT and various deletion mutants in the INT domain of MgcRacGAP in HeLa cells. Cells were transfected with expression vectors carrying Flag-tagged WT or various deletion mutants in the INT domain. After 36 h, cells were immunostained with the anti-Flag Ab (green) and DAPI (blue) and viewed with a fluorescence microscope IX70 (Olympus). Bar, 10 μm. (D) Localization of GFP-fused NLS of MgcRacGAP. GFP-fused aa182-200 of MgcRacGAP, aa182-200(182AAA/199AA), and large T antigen-NLS were expressed in HeLa cells. After 36 h, living cells were viewed with a fluorescence IX70 microscope (Olympus). Bar, 10 μm.